



CMS-BPH-10-010

CERN-PH-EP/2010-093
2024/11/26

Measurement of $B\bar{B}$ Angular Correlations based on Secondary Vertex Reconstruction at $\sqrt{s} = 7$ TeV

The CMS Collaboration*

Abstract

A measurement of the angular correlations between beauty and anti-beauty hadrons ($B\bar{B}$) produced in pp collisions at a centre-of-mass energy of 7 TeV at the CERN LHC is presented, probing for the first time the region of small angular separation. The B hadrons are identified by the presence of displaced secondary vertices from their decays. The B hadron angular separation is reconstructed from the decay vertices and the primary-interaction vertex. The differential $B\bar{B}$ production cross section, measured from a data sample collected by CMS and corresponding to an integrated luminosity of 3.1 pb^{-1} , shows that a sizable fraction of the $B\bar{B}$ pairs are produced with small opening angles. These studies provide a test of QCD and further insight into the dynamics of bb production.

Submitted to the Journal of High Energy Physics

*See Appendix A for the list of collaboration members

1 Introduction

Beauty quarks are abundantly produced through strong interactions in $p\bar{p}$ collisions at the CERN Large Hadron Collider (LHC). The hadroproduction of $b\bar{b}$ pairs is measured to have a large cross section (of the order of $100 \mu b$) at a centre-of-mass energy of 7 TeV [1–3]. Detailed b quark production studies provide substantial information about the dynamics of the underlying hard scattering subprocesses within perturbative Quantum Chromodynamics (pQCD). In lowest order pQCD, i.e. in $2 \rightarrow 2$ parton interaction subprocesses, momentum conservation requires the b and \bar{b} quarks to be emitted in a back-to-back topology. However, higher order $2 \rightarrow 2 + n$ ($n \geq 1$) subprocesses with additional partons (notably gluons) emitted, give rise to different topologies of the final state b quarks. Consequently, measurements of $b\bar{b}$ angular and momentum correlations provide information about the underlying production subprocesses and allow for a sensitive test of pQCD leading-order (LO) and next-to-leading order (NLO) cross sections and their evolution with event energy scales. Studies of b quark production at the LHC may provide insight into the hadronisation properties of heavy quarks at these new energy scales, as well as better knowledge of the heavy quark content of the proton. In addition, identification of b quarks and precision measurements of their properties are crucial ingredients for new physics searches in which $b\bar{b}$ hadroproduction is expected to be one of the main backgrounds.

In this paper, angular correlations between pairs of beauty hadrons, hereafter referred to as “B hadrons”, are studied with the Compact Muon Solenoid (CMS) detector, probing for the first time the region of very small angular separation at $\sqrt{s} = 7$ TeV. Measurements of $B\bar{B}$ -pair production are presented differentially as a function of the opening angle for different event scales, characterised by the leading jet transverse momentum. The extrapolation back to the angular separation of the b quarks, which requires modeling of heavy quark fragmentation and hadronisation, is not considered in this analysis. The results are given for the visible kinematic range defined by the phase space at the hadron level.

Measurements of the full range of $B\bar{B}$ angular separation demand good angular resolution and require the ability to resolve small opening angles when the two B hadrons are inside a single reconstructed jet. The kinematic properties of B hadrons can be reconstructed using jets, leptons from semileptonic decays of B hadrons or secondary vertices (SV) originating from the decay of long-lived B hadrons. In this analysis, a method based on an iterative inclusive secondary vertex finder that exploits the excellent tracking capabilities of the CMS detector is introduced. One advantage of this method is the unique capability to detect $B\bar{B}$ pairs even at small opening angles, in which case the decay products of the B hadrons tend to be merged into a single jet and the standard B jet tagging techniques [4] are not applicable. Previously, studies of azimuthal $b\bar{b}$ correlations using vertexing have been done at lower energy in $p\bar{p}$ collisions [5, 6].

In Section 2, a brief overview of the subdetectors relevant for this analysis is given. Section 3 describes the Monte Carlo (MC) simulations and the programs used for QCD predictions. The event selection, the analysis details, and the determination of efficiencies and systematic uncertainties are described in Section 4. In Section 5 we present the results and compare the data with theoretical predictions.

2 The CMS Detector

A detailed description of the CMS detector can be found in Ref. [7]. The central feature of the CMS apparatus is a superconducting solenoid of 6 m internal diameter, with a 3.8 T axial magnetic field. The subdetectors used in the present analysis are tracking detectors and

calorimeters, located within the field volume. The tracker consists of a silicon pixel and silicon strip tracker covering the pseudorapidity range $|\eta| < 2.5$. The pixel tracker consists of three barrel layers and two endcap disks at each barrel end. The strip tracker has 10 barrel layers and 12 endcap disks. The barrel and endcap calorimeters ($|\eta| < 3$) consist of a lead-tungstate crystal electromagnetic calorimeter (ECAL) and a brass/scintillator hadron calorimeter (HCAL). The ECAL and HCAL cells are grouped into towers, projecting radially outward from the interaction region, for triggering purposes and to facilitate jet reconstruction. The CMS experiment uses a right-handed coordinate system, with the origin at the nominal proton-proton collision point, the x -axis pointing towards the centre of the LHC ring, the y -axis pointing upwards (perpendicular to the LHC plane), and the z -axis pointing along the anticlockwise beam direction. The polar angle θ is measured from the positive z -axis and the azimuthal angle ϕ is measured from the positive x -axis in the xy plane. The radius r denotes the distance from the z -axis and the pseudorapidity is defined by $\eta = -\ln(\tan(\theta/2))$.

3 Monte Carlo Simulation and QCD Predictions

Different simulation programs at the LO and the NLO level have been utilized to describe the b production process within perturbative QCD. Within the LO picture, three parton level production subprocesses can be defined [8, 9], conventionally denoted by flavour creation (FCR), flavour excitation (FEX) and gluon splitting (GSP), and are implemented in Monte Carlo event generators like PYTHIA [10] and HERWIG [11]. These subprocesses are related to different final state topologies. Notably, in FCR processes the $b\bar{b}$ pairs are expected to be emitted in a back-to-back topology, which corresponds to a large angular separation between the b and \bar{b} quarks, whereas in GSP the pair emission follows a more collinear topology, i.e. a small angular separation between the b and \bar{b} quarks. At higher orders in QCD, the FCR, FEX and GSP separation of production subprocesses becomes meaningless and only the combination of the $2 \rightarrow 2$ and $2 \rightarrow 2 + n$ ($n \geq 1$) subprocesses is relevant. Calculations of such processes are implemented in MC@NLO [12–14] or FONLL [15]. The MADGRAPH/MADEVENT [16, 17] generator provides the possibility to simulate $2 \rightarrow 2, 3$ subprocesses at tree-level, providing a hybrid solution between $2 \rightarrow 2$ at LO and the NLO simulations. We use also the CASCADE [18] generator, which is based on off-shell LO matrix elements using high-energy factorization [19] convolved with unintegrated parton distributions.

The basic Monte Carlo event generator applied in this analysis is the LO PYTHIA program (version 6.422 [10]), which is used to determine selection efficiencies and to optimise the vertexing algorithm for B hadron reconstruction. The event samples are generated applying the standard PYTHIA settings [10] with tune D6T [20] for the underlying event and with the CTEQ6L1 [21] proton parton distribution functions (PDF). All events generated by the PYTHIA program are processed with a detailed simulation of the CMS detector response based on the GEANT4 package [22].

For comparison with theoretical predictions, events with two and three partons in the final state are generated by means of the MADGRAPH/MADEVENT4 program, where the showering is performed with PYTHIA, and the jet matching scheme used is “ k_T -MLM” [23]. The CTEQ6L1 [21] parton distribution functions are used, and the mass of the b quark is set to $m_b = 4.75$ GeV.

For the events produced with the CASCADE generator, the CCFM set A [24] of parton distributions is used. The calculations include the processes $g^*g^* \rightarrow b\bar{b}$ and $g^*q \rightarrow gq \rightarrow b\bar{b}X$. The matrix element of $g^*g^* \rightarrow b\bar{b}$ already includes a large fraction of the process $g^*g \rightarrow gg \rightarrow b\bar{b}X$ [19, 25], therefore $g^*g \rightarrow gg \rightarrow b\bar{b}X$ is not added to avoid double counting.

A further set of QCD events is produced by means of the MC@NLO generator (version 3.4 [14] with standard scale settings and b-quark mass $m_b = 4.75$ GeV), which matches NLO QCD matrix element calculations with parton shower simulations as implemented in HERWIG (version 6.510) [11]. The proton PDF set used is CTEQ6M [21]. For the NLO generated events, no full CMS detector simulation is done. Subsequent to the parton showering and hadronisation process, the generated stable particles in the events are clustered into jets with the anti- k_T jet algorithm [26].

4 Event Selection and Data Analysis

The data sample used in this analysis was collected by the CMS experiment during 2010 at a centre-of-mass energy of $\sqrt{s} = 7$ TeV and corresponds to an integrated luminosity of $3.1 \pm 0.3 \text{ pb}^{-1}$. Only data from runs when the CMS detector components relevant for this analysis were fully functional and when stable beam conditions were present are used. Events from non-collision processes are rejected by requiring a primary (“collision”) vertex (PV) [27, 28] with at least four well reconstructed tracks. Background from beam-wall and beam halo events, and events faking high energy deposits in the HCAL, are filtered out based on pulse shape, hit multiplicity and timing criteria.

4.1 Analysis Overview

The analysis relies on the single-jet trigger in both the hardware-level (L1) and the software high-level (HLT) components of the CMS trigger system [7]. We require at least one HLT jet with uncorrected transverse calorimetric energy E_T^U above a trigger threshold of 15, 30 or 50 GeV. Figure 1 shows the leading jet transverse momentum (p_T) spectra with particle flow jets [29] and the corresponding trigger efficiency dependence on p_T . The efficiencies, also shown in Figure 1, are determined using events selected with a lower E_T^U (prescaled) trigger.

The event sample is then divided into three energy scale bins corresponding to the p_T ranges where the different jet triggers are over 99% efficient. These correspond to samples where the transverse momenta of the leading jet, using corrected jet energies [30], exceed 56, 84 and 120 GeV, respectively. The effective integrated luminosity, taking into account the trigger prescale factors, corresponds to 0.031, 0.313 and 3.069 pb^{-1} , respectively, for the three samples, including some overlap.

The visible kinematic range for the measurements is defined at the B hadron level by the requirements $|\eta(B)| < 2.0$ and $p_T(B) > 15$ GeV for both of the B hadrons. The leading jet used to define the minimum energy scale is required to be within $|\eta(\text{jet})| < 3.0$.

In this analysis, the HLT triggered events are required to have at least one reconstructed jet with a minimum corrected p_T , a reconstructed PV, and in addition at least two reconstructed secondary vertices (SV). For the offline jet reconstruction, particle flow objects [29] are clustered with the anti- k_T jet algorithm [26, 31] with a distance parameter $R_{k_T} = 0.5$. For further $B\bar{B}$ angular analysis, these generic secondary vertices are required to originate from B hadron decays, as described in the following paragraphs.

The flight direction of the original B hadron is approximated by the vector \overrightarrow{SV} , joining the PV (position of B hadron production) and the SV (position of the B hadron decay). The length $|\overrightarrow{SV}|$ is the three-dimensional flight distance (D_{3D}) and its significance is given by $S_{3D} = D_{3D}/\sigma(D_{3D})$, where $\sigma(D_{3D})$ is the uncertainty of D_{3D} .

In an event with two SVs, which are considered to originate from a $b\bar{b}$ pair, the angular correla-

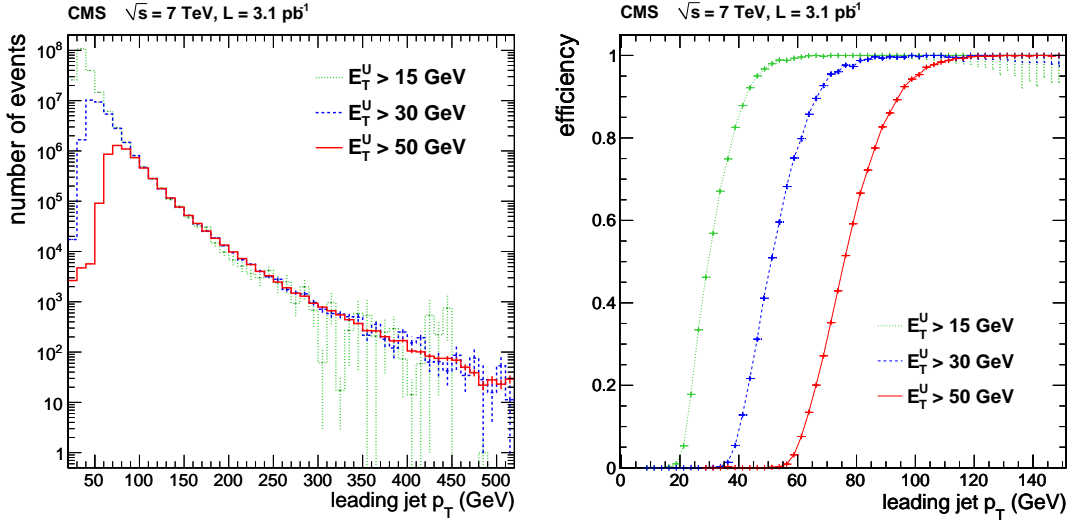


Figure 1: The measured transverse momentum distributions of the leading jet in the event (left) and measured efficiency to trigger an event on the high-level trigger as a function of jet p_T (right), for three different trigger thresholds.

tion variables between the B and \bar{B} hadrons are calculated using their flight directions. Typical variables used for the characterization of the angular correlations between the two hadrons are the difference in azimuthal angles ($\Delta\phi$) and the difference in polar angles, usually expressed in terms of pseudorapidity ($\Delta\eta$), or the combined separation variable $\Delta R = \sqrt{\Delta\eta^2 + \Delta\phi^2}$.

The kinematic regions with $\Delta R < 0.8$ and with $\Delta R > 2.4$ are used for comparisons or normalisations of the simulation. The cross sections integrated over these two regions will be denoted by $\sigma_{\Delta R < 0.8}$ and by $\sigma_{\Delta R > 2.4}$, and the ratio by $\rho_{\Delta R} = \sigma_{\Delta R < 0.8} / \sigma_{\Delta R > 2.4}$. This is inspired by the theoretical predictions, since at low ΔR values the gluon splitting process is expected to contribute significantly, whereas at high ΔR values flavour creation prevails.

4.2 Vertex Reconstruction and B Candidate Identification

The primary vertex is reconstructed from tracks of low impact parameter with respect to the nominal interaction region. In cases of multiple interactions in the same bunch crossing (pile-up events), the primary interaction vertex is chosen to be the one with the largest squared transverse momentum sum $S_T = \sum p_{T,i}^2$, where the sum runs over all tracks associated with the vertex. Residual effects from pile-up events are found to be negligible.

Next, the events are required to have at least two reconstructed secondary vertices. An inclusive secondary vertex finding (IVF) technique, completely independent of jet reconstruction, is applied for this purpose. This technique reconstructs secondary vertices by clustering tracks around the so-called seeding tracks characterized by high three-dimensional impact parameter significance $S_d = d/\sigma(d)$, where d and $\sigma(d)$ are the impact parameter and its uncertainty at the PV, respectively. The tracks are clustered to a seed track based on their compatibility given their separation distance in three dimensions, the separation distance significance (distance normalised to its uncertainty), and the angular separation. The clustered tracks are then fitted to a common vertex with an outlier-resistant fitter [32, 33]. The vertices sharing more than 70% of the tracks compatible within the uncertainties are merged. As a final step, all tracks are assigned to either the primary or the secondary vertices on the basis of the significance of the track to vertex distance.

In this analysis, a SV is required to be made up of at least three tracks, to have a maximal two-

dimensional flight distance $D_{xy} = |\vec{SV}_{xy}| < 2.5$ cm, a minimal two-dimensional flight distance significance $S_{2D} = D_{xy}/\sigma(D_{xy}) > 3$, and to possess a vertex mass $m_{SV} < 6.5$ GeV. Here, $\sigma(D_{xy})$ is the uncertainty on D_{xy} . The four-momentum of the vertex $p_{SV} = (E_{SV}, \vec{p}_{SV})$ is calculated as the sum $p_{SV} = \sum p_i$ over all tracks fitted to that vertex, with $p_i = (E_i, \vec{p}_i)$, using the pion mass hypothesis for every track to obtain its energy E_i . The vertex mass m_{SV} is calculated as $m_{SV}^2 = E_{SV}^2 - \vec{p}_{SV}^2$. The four-momentum of the reconstructed B hadron candidate is then identified with the SV four-momentum, and thus the variables $p_T(B), \eta(B)$ for the B hadron candidates are readily calculated from p_{SV} .

Events with at least two secondary vertices may originate from any of the following processes: a) true ‘signal’ $B\bar{B}$ events; b) true $B\bar{B}$ events where at least one B hadron is not correctly reconstructed (SV from other sources); c) QCD events with light quark and gluon jets, which enter through misidentification of vertices not originating from B decay; d) direct $c\bar{c}$ production with long lived D hadrons; e) sequential $B \rightarrow D \rightarrow X$ decay chains, where B hadrons decay to long lived D hadrons, and both B and D vertices are reconstructed. The $B\bar{B}$ signal events contain a fraction from top quark pair production of less than 1% [34, 35].

Often, both the B and D decay vertices are reconstructed by the IVF. Such topologies need to be distinguished from events with two quasi-collinear B hadrons. To achieve this, an iterative merging procedure is applied to vertices with $\Delta R < 0.4$. The procedure is optimised to yield a single B candidate associated with a decay chain $B \rightarrow D \rightarrow X$, while successfully retaining two B candidates also in events where two real B hadrons are emitted nearly collinearly. The vertices are merged into a single B candidate if the invariant mass of the sum over all tracks is below 5.5 GeV and $\cos \beta > 0.99$, where β is the angle between the line connecting the two vertices and the sum of the momenta of the tracks associated to the vertex at largest distance from the PV.

All B candidates are retained if they have a minimal 3D flight distance significance $S_{3D} > 5$, a pseudorapidity $|\eta(SV)| < 2$, a transverse momentum $p_T(SV) > 8$ GeV, and a vertex mass $m_{SV} > 1.4$ GeV. The quality of the B candidate reconstruction technique is illustrated in Fig. 2 for events with a leading jet having $p_T > 84$ GeV (all selection cuts apart from those on the shown quantities are applied). The simulation describes the data very well in terms of vertex mass and 3D decay length significance distribution.

Only those events which have exactly two B hadron candidates and which have a vertex mass sum $m_1 + m_2 > 4.5$ GeV are retained. A total of 160, 380 and 1038 events pass all these requirements for the three leading jet p_T bins, respectively from the lowest to the highest. The overall contributions from events with three or more B candidates is found to be negligible (less than 1%).

4.3 Efficiency and Resolution

This analysis uses selection efficiency corrections as a function of the leading jet p_T and the ΔR between the two SVs. The corrections are determined from the simulated PYTHIA event samples. They extrapolate from the measured vertex momenta to the visible phase space of true B hadrons, defined by $|\eta(B)| < 2.0$, and $p_T(B) > 15$ GeV. The momentum measured by the vertex candidate represents of the order of 50% of the true B hadron momentum. The overall event reconstruction efficiencies (including both B hadron decays) are found to be 7.4%, 9.3% and 10.7%, on average, for the three jet p_T bins, respectively from the lowest to the highest.

The validity of the ΔR -dependence of the efficiencies obtained from simulation is checked using a data driven method based on event mixing, as illustrated below. It is found that the ΔR -

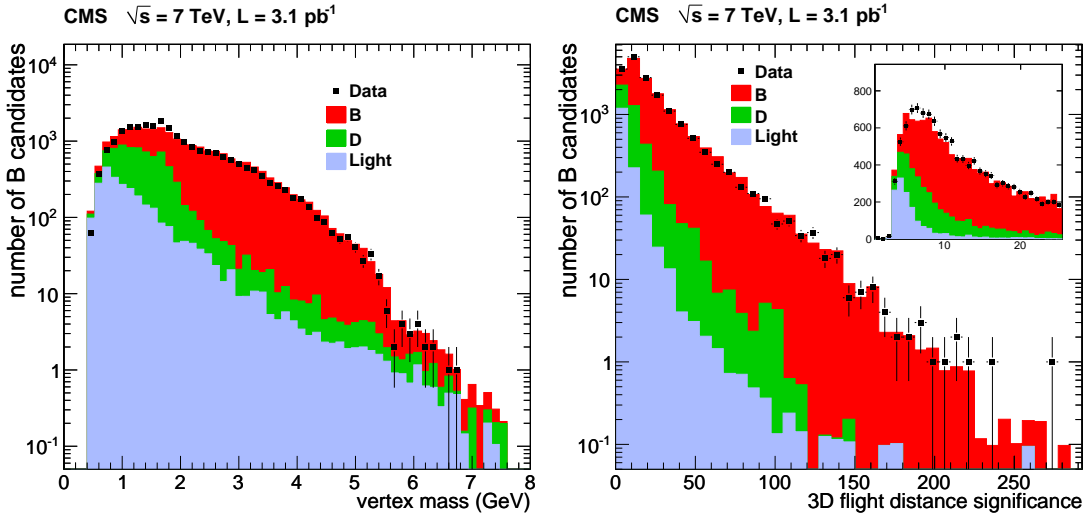


Figure 2: Properties of the reconstructed B candidates: vertex mass distribution (left) and flight distance significance distribution (right). The inset in the right plot shows a zoom of the flight distance significance distribution with narrower bins and linear scale. The data are shown by the solid points. The decomposition into the different sources, beauty, charm and light quarks, is shown for the PYTHIA Monte Carlo simulation. The simulated distributions are normalised to the total number of data events. All selection cuts apart from those on the shown quantities are applied.

dependence is well described by the simulation, justifying this approach. The differences are used to estimate the systematic uncertainties.

The resolution achieved in the ΔR reconstruction is estimated from simulation. The comparison of the ΔR values reconstructed between the two vertices ΔR_{VV} with the values calculated between the original true B hadrons ΔR_{BB} , determines the resolution. This is illustrated in Fig. 3, which shows the two-dimensional distribution ΔR_{VV} versus ΔR_{BB} and its projection onto the diagonal ($\Delta R_{VV} - \Delta R_{BB}$). A fit to this projection directly yields an average resolution better than 0.02 in ΔR for the core region, a value much smaller than the ΔR bin width of 0.4.

In order to calculate differential cross sections, a ΔR -dependent purity correction is applied. The contributions to purity due to migration are illustrated in Fig. 3a. The total number of event entries off the diagonal is found to be about 3%. The largest impurity occurs close to $\Delta R_{VV} \approx 3$ as can be seen in the 2D plot. These events are due to misreconstructed collinear events where only one B hadron is reconstructed, while a fake vertex is found in the recoiling light quark jet. The largest effect on a single bin is below 10% and this is taken into account in the purity correction. The uncertainty arising from this correction is included in the systematic uncertainties. The average $B\bar{B}$ purity is found to be 84%, with a variation within about $\pm 10\%$ over the full ΔR range in the visible region for the three leading jet p_T bins.

4.4 Systematic Uncertainties

Uncertainties relevant to the shape of the differential distributions are crucial for this paper. The consistency in shape between the data and the simulation is assessed and the systematic uncertainties are estimated by data driven methods. The systematic uncertainties related to the absolute normalisation are much larger than the shape dependent ones. They sum up to a total of 47%, but do not affect the shape analysis (see below). The dominant contribution originates from the B hadron reconstruction efficiency ($\pm 20\%$, estimated in [4]), which amounts to a total

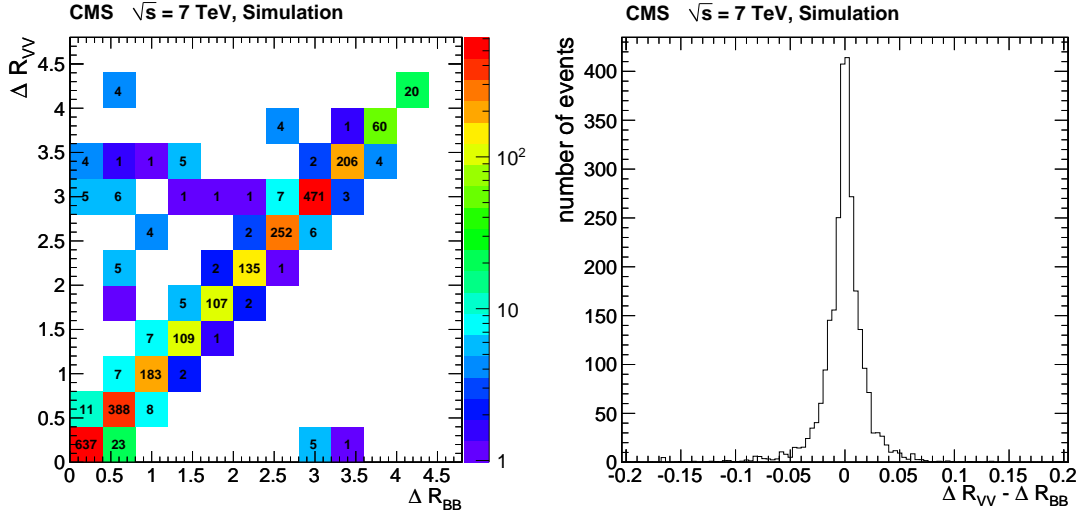


Figure 3: Resolution of the ΔR reconstruction, obtained using simulation for the leading jet $p_T > 84$ GeV sample. Left: ΔR values reconstructed between the two secondary vertices ΔR_{VV} versus the values between the original B hadrons ΔR_{BB} , in the visible B hadron phase space (see text). Right: projection onto the diagonal ($\Delta R_{VV} - \Delta R_{BB}$). The numbers in the boxes represent the number of events reconstructed in that particular bin.

of 44% for reconstructing two B hadrons.

In the following the shape dependent systematic uncertainties for the ΔR distributions are discussed. The values are quoted in terms of the relative change of the integrated cross section ratio $\rho_{\Delta R} = \sigma_{\Delta R < 0.8} / \sigma_{\Delta R > 2.4}$. Very similar systematic uncertainties arise for the $\Delta\phi$ distributions and, hence, they are not quoted separately.

- *Algorithmic effects.* The shape of the ΔR dependence of the efficiency $\alpha(\Delta R)$ is checked by means of an event mixing method. This event mixing technique mimics an event with two genuine SVs by merging two independent events, where each has at least one reconstructed SV. The positions of the two PVs are required to be within $20\ \mu\text{m}$ in three-dimensional space. This mixed event is then analysed and the fraction of cases where both original SVs are again properly reconstructed is used to determine the ΔR dependence of the efficiency to find two genuine SVs in an event which had the SVs already reconstructed. The shape of this efficiency $\alpha(\Delta R)$ is determined for the data and for the simulated samples independently in bins of ΔR . The vertex reconstruction efficiency as a function of ΔR for data and for simulation, and their ratio are shown in Fig. 4. Since in this analysis the shape is the most relevant property, the values in Fig. 4b have been rescaled to the mean value. This ratio exhibits good consistency in shape between simulation and data over the full ΔR range, including the region of small ΔR . The differences are found to be within 2% and are taken as systematic uncertainties.
- *B hadron momenta.* The mean reconstruction efficiency for an observed ΔR value strongly depends on the kinematic properties of the B hadron pair. It depends on the p_T of each B hadron and predominantly on the softer of the two. Since all efficiency corrections are taken from the MC simulation, it is important to verify that the kinematic behaviour of the $B\bar{B}$ pairs is also properly modelled by the simulation. Confidence in the Monte Carlo modelling is provided by comparing the transverse momentum distributions of the reconstructed B candidates derived from data and from Monte Carlo simulation. The distributions of the reconstructed p_T of the harder

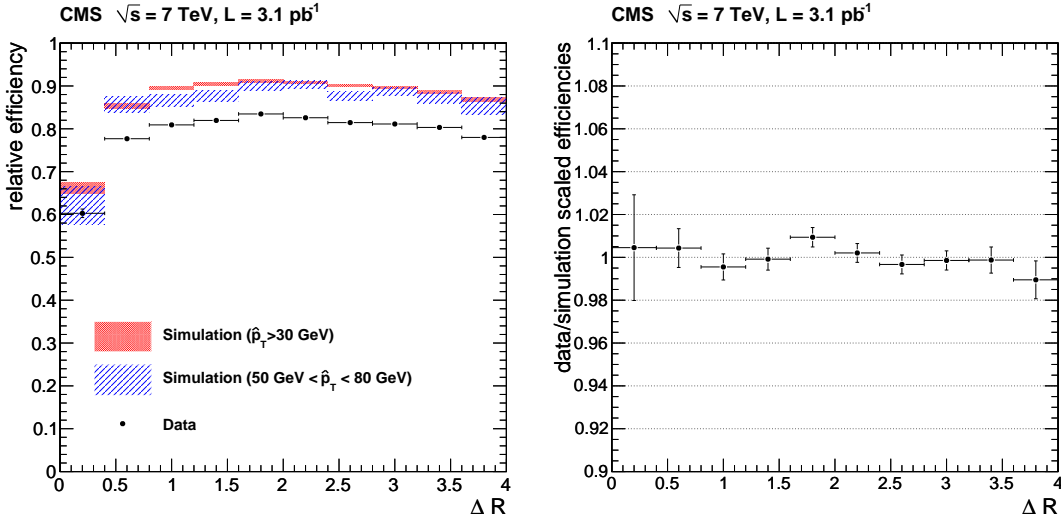


Figure 4: Study of the vertex reconstruction efficiency by the event mixing method. Shown as a function of ΔR are the relative vertex reconstruction efficiency (left) $\alpha(\Delta R)$ (see text), and the ratio (right) between the quantities $\alpha(\Delta R)$ determined from the data and from the simulation. The simulated $\alpha(\Delta R)$ distribution (left) is shown for two energy scales, characterized by \hat{p}_T , the PYTHIA parameter describing the transverse momentum in the hard subprocess. The ratio (right) is rescaled to unity to estimate the accuracy of the simulated shape.

and of the softer of the two hadrons, their asymmetry, as well as the ΔR dependence of the average reconstructed p_T of the softer hadron for the three leading jet p_T regions, are shown in Fig. 5. The differences between the data and the simulation, convolved with the p_T -dependent efficiency, are found to have an effect on the final result of between 4% and 8%. These values are used to estimate the systematic uncertainties reported in Table 1 as “B hadron kinematics”.

- *Uncertainty on the Jet Energy Scale (JES).* The JES influences the ΔR shape of the two B hadrons. Its effect on the p_T of the leading jet is estimated assuming a linear rise of the p_T dependency of the relative cross section ratio (see below). Given that the higher p_T scales exhibit a larger relative contribution to the cross section at low ΔR , the actual ΔR shape is distorted by this effect. The uncertainty on the JES is determined by assuming a $\pm 3\%$ [30] uncertainty on average for the energy region relevant for this analysis. An additional $\pm 5\%$ is added to take into account the differences in the jet energy corrections between b and light jets as estimated in the simulation. This yields a variation in the ΔR shape within 6%, which is taken as systematic uncertainty.
- *Phase space correction.* The measurements of vertices are corrected to the visible phase space of the B hadrons defined by $|\eta(B)| < 2.0$ and $p_T(B) > 15 \text{ GeV}$, using the PYTHIA Monte Carlo simulation. In the analysis only reconstructed B hadrons above a p_T of 8 GeV are considered. The uncertainty arising from this choice has been estimated by varying the p_T cut on the reconstructed vertex from 8 to 10 GeV, re-computing the MC correction and repeating the final measurement. The uncertainty is found to be 2.8%.
- *Migration.* The bin-to-bin migrations in the sample are small because, as shown in Fig. 3, the core of the vertex resolution in ΔR (0.02) is much smaller than the chosen bin width (0.4). The migrations are taken into account through the efficiency corrections. The off-diagonal contributions (predominantly at $\Delta R_{VV} \approx \pi$ from mis-

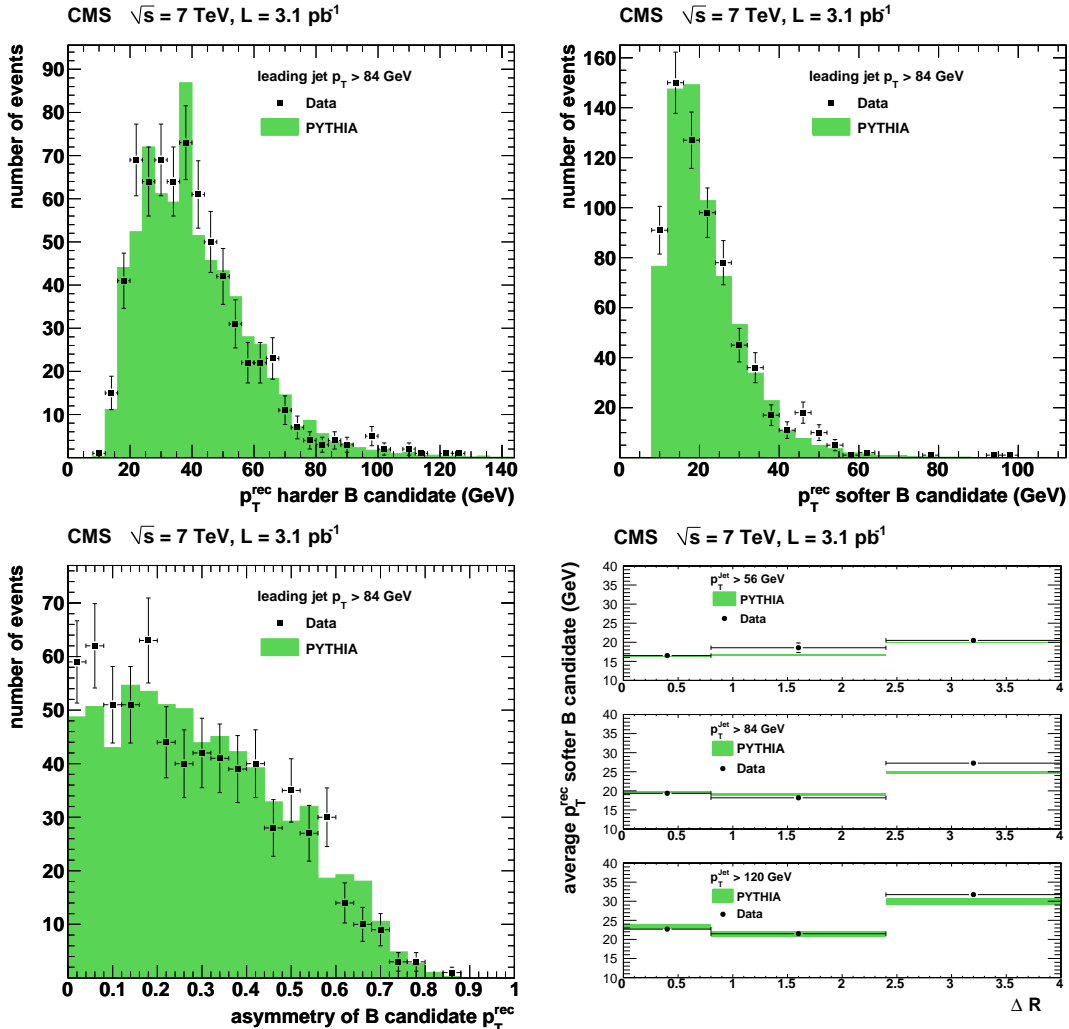


Figure 5: Distributions of the reconstructed p_T of the two B hadrons: p_T of the harder B hadron (top left); p_T of the softer B hadron (top right); asymmetry (bottom left) of the p_T of the harder and the softer B hadron; average p_T (bottom right) of the softer B hadron as a function of ΔR for data (solid dots) and PYTHIA simulation (green bars) for the three leading jet p_T regions.

reconstructed collinear gluon splitting events, with one vertex from the recoiling jet) are subtracted on a bin-to-bin basis. An uncertainty of up to 2.1% on this purity correction is obtained by increasing the small angle $\Delta R < 0.8$ contribution by 50% (compatible with the measured results, as presented below).

- *Monte Carlo statistics.* An additional bin-to-bin systematic uncertainty results from the limited number of simulated events. An uncertainty of 13% is used, conservatively taking the maximum value of either the statistical uncertainty of the simulation or half of the largest bin-to-bin fluctuation observed in the correction function between any of the ΔR bins. This uncertainty is mostly relevant for Figs. 6 and 8; its effect is reduced in Fig. 7.

The shape-dependent systematic uncertainties are calculated and included binwise in the figures, as indicated by the outer error bars which show statistical and systematic uncertainties added in quadrature. They are summarised in Table 1. The overall normalisation uncertainties are not included in the error bars in the figures.

Table 1: Systematic uncertainties affecting the shape of the differential cross section as a function of ΔR , for the three leading jet p_T regions. The values are quoted in terms of percentage changes of the integrated cross section ratio $\rho_{\Delta R}$. In the figures, these values are included for each bin. Very similar systematic uncertainties are assumed for the $\Delta\phi$ distributions.

Source of uncertainty in shape	Change in $\rho_{\Delta R} = \sigma_{\Delta R < 0.8} / \sigma_{\Delta R > 2.4}$ (%)		
	Leading jet p_T bin (GeV)		
	> 56	> 84	> 120
Algorithmic effects (data mixing)	2.0	2.0	2.0
B hadron kinematics (p_T of softer B)	8.0	7.0	4.0
Jet energy scale	6.0	6.0	6.0
Phase space correction	2.8	2.8	2.8
Bin migration from resolution	0.6	1.3	2.1
Subtotal shape uncertainty	10.6	9.9	8.3
MC statistical uncertainty	13.0	13.0	13.0
Total shape uncertainty	16.8	16.4	15.4

5 Results

5.1 Differential Distributions in ΔR and $\Delta\phi$

The differential cross section of $B\bar{B}$ -pair production is measured as a function of the angular separation variables ΔR and $\Delta\phi$ between the two reconstructed B hadrons for three different energy scales. The results are presented for the visible kinematic phase space of the B hadrons and the leading jet p_T ranges as defined in Section 4.1. The cross sections are determined by applying efficiency corrections and normalising to the total integrated luminosity, according to

$$\left(\frac{d\sigma_{\text{visible}}(pp \rightarrow B\bar{B} X)}{dA} \right)_i = \frac{N_i(\text{data}) \cdot f_i}{\Delta A_i \cdot \mathcal{L} \cdot \epsilon_i}, \quad (1)$$

where $N_i(\text{data})$ denotes the number of selected signal $B\bar{B}$ events in bin i , \mathcal{L} the integrated luminosity, ϵ_i the total efficiency, f_i the purity correction factor, and ΔA_i the width of bin i in variable A , with A being ΔR or $\Delta\phi$.

The measured cross sections are shown in Fig. 6 as a function of ΔR and $\Delta\phi$ for the three leading jet p_T regions. The error bars on the data points include statistical and uncorrelated systematic uncertainties. An uncertainty of 47% common to all data points due to the absolute normalisation is not shown in the figure. The bars shown for the PYTHIA simulation in Fig. 6 are normalised to the region $\Delta R > 2.4$ or $\Delta\phi > 2.4$, where the theory calculations are expected to be more reliable, since the cross section is anticipated to be dominated by leading order diagrams (flavour creation).

It is interesting to note that the cross sections at small values of ΔR or $\Delta\phi$ are found to be substantial. They exceed the cross sections observed at large angular separation values, the configuration where the two B hadrons are emitted in opposite directions.

The scale dependence is illustrated in Table 2 and Fig. 7, where the left panel shows the ratio

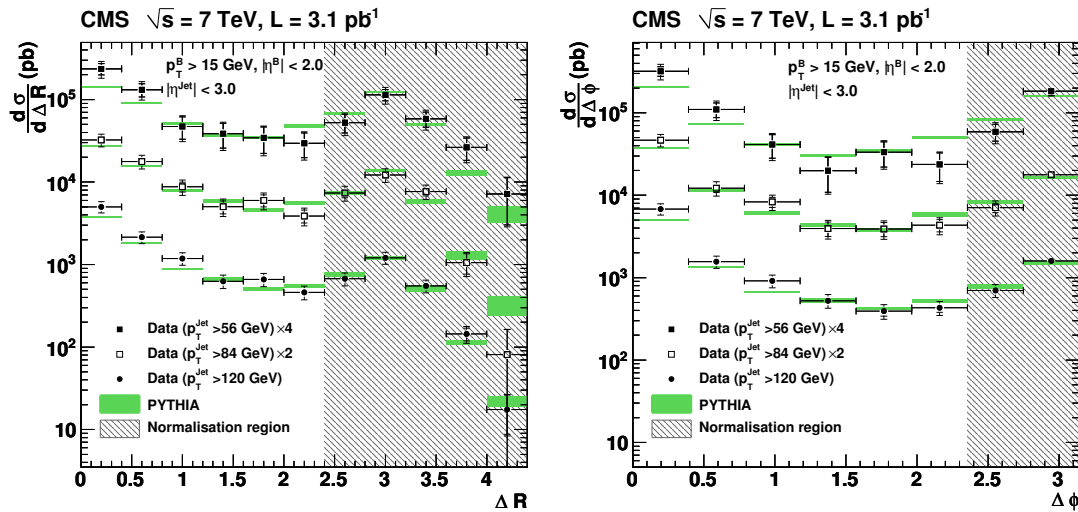


Figure 6: Differential $B\bar{B}$ production cross sections as a function of ΔR (left) and $\Delta\phi$ (right) for the three leading jet p_T regions. For clarity, the $p_T > 56$ and 84 GeV bins are offset by a factor 4 and 2, respectively. For the data points, the error bars show the statistical (inner bars) and the total (outer bars) uncertainties. A common uncertainty of 47% due to the absolute normalisation on the data points is not included. The symbols denote the values averaged over the bins and are plotted at the bin centres. The PYTHIA simulation (shaded bars) is normalised to the region $\Delta R > 2.4$ or $\Delta\phi > 2.4$, as indicated by the shaded normalisation regions. The widths of the shaded bands indicate the statistical uncertainties of the predictions.

$\rho_{\Delta R}$ as a function of the leading jet p_T , a measure of the hard interaction scale. The right panel shows the asymmetry of the cross section contributions between small and large ΔR values, $(\sigma_{\Delta R < 0.8} - \sigma_{\Delta R > 2.4}) / (\sigma_{\Delta R < 0.8} + \sigma_{\Delta R > 2.4})$. The measured data clearly indicate that the relative contributions of $\sigma_{\Delta R < 0.8}$ significantly exceed those of $\sigma_{\Delta R > 2.4}$. In addition, the data show that this excess depends on the energy scale, increasing towards larger leading jet p_T values.

Table 2: p_T cut of the leading jet, average jet p_T , cross sections in the two ΔR regions (including the 47% uncertainty on the absolute normalisation), average efficiency, average purity, and cross section ratio for the data, as well as for the PYTHIA and MADGRAPH simulations. Statistical and systematic uncertainties are included for the data, while for the simulations only the statistical uncertainties are given.

Jet p_T		$\rho_{\Delta R} = \sigma_{\Delta R < 0.8} / \sigma_{\Delta R > 2.4}$						
Cut (GeV)	$\langle p_T \rangle$ (GeV)	$\sigma_{\Delta R < 0.8}$ (nb)	$\sigma_{\Delta R > 2.4}$ (nb)	$\langle \epsilon \rangle$ (%)	$\langle P \rangle$ (%)	Data (stat+sys)	PYTHIA (stat)	MADGRAPH (stat)
> 56	72	37 ± 26	26 ± 16	7.4	84.9	1.42 ± 0.29	0.89 ± 0.02	1.53 ± 0.07
> 84	106	10 ± 4	5.6 ± 4.0	9.3	84.6	1.77 ± 0.26	1.51 ± 0.05	2.60 ± 0.09
> 120	150	2.8 ± 1.0	1.0 ± 1.2	10.7	83.2	2.74 ± 0.32	2.13 ± 0.07	3.64 ± 0.11

5.2 Comparisons with Theoretical Predictions

The measured distributions are compared with various theoretical predictions, based on perturbative QCD calculations, both at LO and NLO.

Within pQCD, a back-to-back configuration for the production of the $B\bar{B}$ pair (i.e. large values of ΔR and/or $\Delta\phi$) is expected for the LO processes, while the region of phase space with small opening angles between the B and \bar{B} hadrons provides strong sensitivity to collinear emission processes. The higher-order processes, such as gluon radiation which splits into $b\bar{b}$ pairs, are

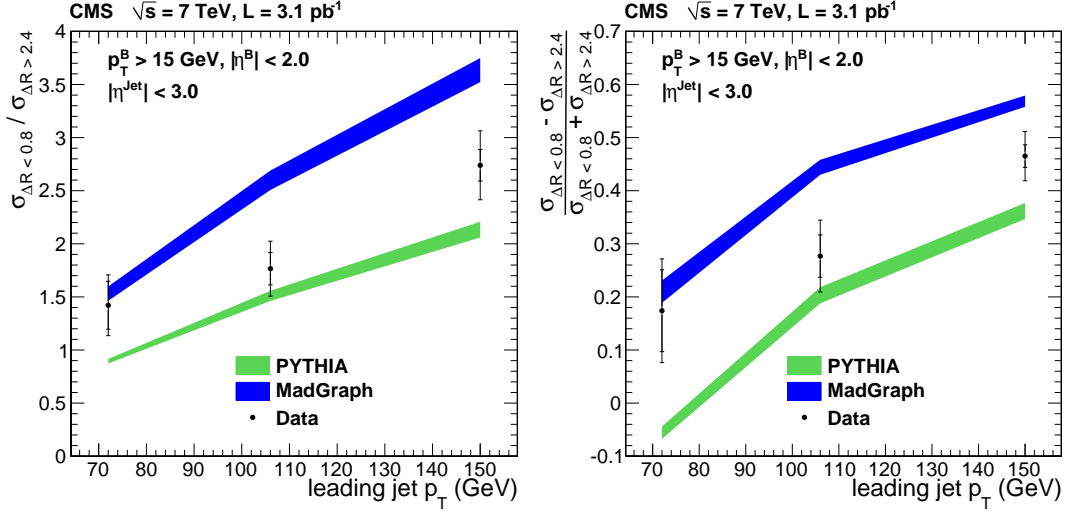


Figure 7: Left: ratio between the $B\bar{B}$ production cross sections in $\Delta R < 0.8$ and $\Delta R > 2.4$, $\rho_{\Delta R} = \sigma_{\Delta R < 0.8} / \sigma_{\Delta R > 2.4}$, as a function of the leading jet p_T . Right: asymmetry between the two regions, $(\sigma_{\Delta R < 0.8} - \sigma_{\Delta R > 2.4}) / (\sigma_{\Delta R < 0.8} + \sigma_{\Delta R > 2.4})$. The symbols denote the data averaged over the bins and are plotted at the mean leading jet p_T of the bins. For the data points, the error bars show the statistical (inner bars) and the total (outer bars) errors. Also shown are the predictions from the PYTHIA and MADGRAPH simulations, where the widths of the bands indicate the uncertainties arising from the limited number of simulated events.

anticipated to have a smaller angular separation between the b quarks. Naively, the flavour creation contribution is expected to be dominant in most regions of the phase space, whereas the gluon splitting contributions should be relatively small.

The measurements show that the $B\bar{B}$ production cross section ratio $\rho_{\Delta R}$ increases as a function of the leading jet p_T in the event (see Fig. 7). Larger p_T values lead to more gluon radiation and, hence, are expected to produce more gluon splitting into $B\bar{B}$ pairs. This general trend is described by the theoretical calculations.

In order to provide a detailed comparison between the data and the theory predictions in terms of shape, Fig. 8 presents the ratios, of the data as well as of the MADGRAPH, MC@NLO and CASCADE models, with respect to the PYTHIA predictions, for the three different scales in leading jet p_T . The values for the PYTHIA simulation are normalised in the region $\Delta R > 2.4$ (or $\Delta\phi > 2.4$).

It is observed that none of the predictions describes the data very well. The data lie between the MADGRAPH and the PYTHIA curves. The MC@NLO calculations do not describe the shape of the observed ΔR distribution. In particular, at small values of ΔR , where higher-order processes, notably gluon splitting, are expected to be large, the MC@NLO predictions are substantially below the data. The $\Delta\phi$ distribution is more adequately reproduced by MC@NLO. The CASCADE predictions are significantly below the data in all regions, both in the ΔR and $\Delta\phi$ distributions.

6 Summary

A first measurement of the angular correlations between $B\bar{B}$ pairs produced in pp collisions at a centre-of-mass energy of 7 TeV is presented. The measurements are based on data corresponding to an integrated luminosity of $3.1 \pm 0.3 \text{ pb}^{-1}$ recorded by the CMS experiment during 2010. The detection of the B hadrons is based on the reconstruction of the secondary vertices from

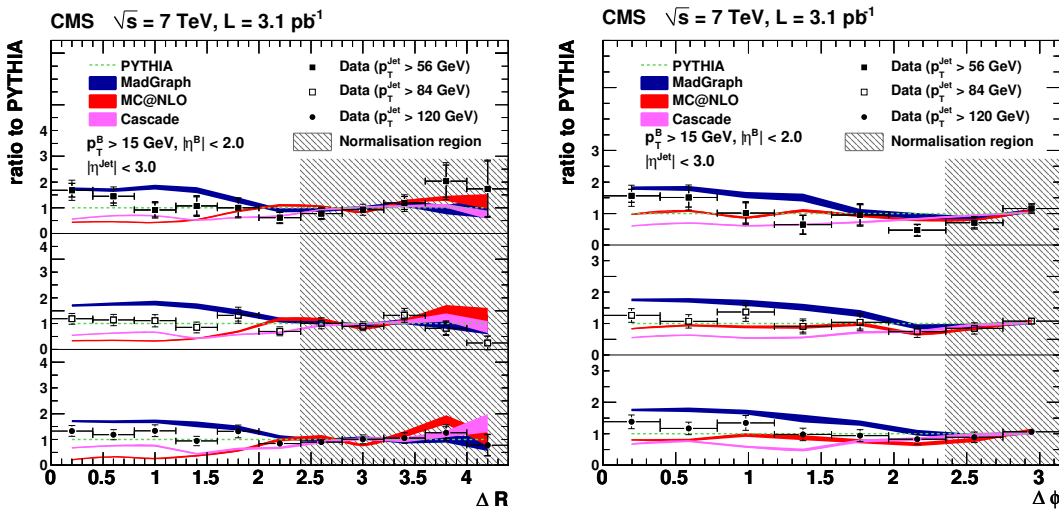


Figure 8: Ratio of the differential $B\bar{B}$ production cross sections, as a function of ΔR (left) and $\Delta\phi$ (right), for data, MADGRAPH, MC@NLO and CASCADE, with respect to the PYTHIA predictions, for the three leading jet p_T bins. The simulation is normalised to the region $\Delta R > 2.4$ and $\Delta\phi > 2.4$ (FCR region), as indicated by the shaded normalisation region. The widths of the theory bands indicate the statistical uncertainties of the simulation.

their decays. The results are given in terms of normalised differential production cross sections as functions of the angular separation variables ΔR and $\Delta\phi$ between the two B hadrons. The data exhibit a substantial enhancement of the cross section at small angular separation, exceeding the values measured at large ΔR and $\Delta\phi$. The fraction of cross section in this collinear region is found to increase with the leading jet p_T of the event.

The measurements are compared to predictions, based on LO and NLO perturbative QCD calculations. Overall, it is found that the data lie between the MADGRAPH and the PYTHIA predictions. Neither the MC@NLO nor the CASCADE calculations describe the shape of the ΔR distribution well. In particular the collinear region at small values of ΔR , where the contributions of gluon splitting processes are expected to be large, is not adequately described by any of the predictions.

Acknowledgements

We wish to congratulate our colleagues in the CERN accelerator departments for the excellent performance of the LHC machine. We thank the technical and administrative staff at CERN and other CMS institutes, and acknowledge support from: FMSR (Austria); FNRS and FWO (Belgium); CNPq, CAPES, FAPERJ, and FAPESP (Brazil); MES (Bulgaria); CERN; CAS, MoST, and NSFC (China); COLCIENCIAS (Colombia); MSES (Croatia); RPF (Cyprus); Academy of Sciences and NICPB (Estonia); Academy of Finland, ME, and HIP (Finland); CEA and CNRS/IN2P3 (France); BMBF, DFG, and HGF (Germany); GSRT (Greece); OTKA and NKTH (Hungary); DAE and DST (India); IPM (Iran); SFI (Ireland); INFN (Italy); NRF and WCU (Korea); LAS (Lithuania); CINVESTAV, CONACYT, SEP, and UASLP-FAI (Mexico); PAEC (Pakistan); SCSR (Poland); FCT (Portugal); JINR (Armenia, Belarus, Georgia, Ukraine, Uzbekistan); MST and MAE (Russia); MSTD (Serbia); MICINN and CPAN (Spain); Swiss Funding Agencies (Switzerland); NSC (Taipei); TUBITAK and TAEK (Turkey); STFC (United Kingdom); DOE and NSF (USA).

References

- [1] CMS Collaboration, "Inclusive b-hadron Production Cross Section with Muons in pp Collisions at $\sqrt{s} = 7$ TeV", arXiv:1101.3512.
- [2] CMS Collaboration, "Inclusive b -Jet Production in pp Collisions at $\sqrt{s} = 7$ TeV", CMS Note **CERN-CMS-PAS-BPH-10-009** (2010).
- [3] LHCb Collaboration, "Measurement of $\sigma(pp \rightarrow b\bar{b}X)$ at $\sqrt{s} = 7$ TeV in the forward region", *Phys. Lett.* **B694** (2010) 209, arXiv:1009.2731.
doi:10.1016/j.physletb.2010.10.010.
- [4] CMS Collaboration, "Commissioning of b Jet Identification with pp Collisions at $\sqrt{s} = 7$ TeV", CMS Note **CERN-CMS-PAS-BTV-10-001** (2010).
- [5] CDF Collaboration, "Measurements of $b\bar{b}$ azimuthal production correlations in $p\bar{p}$ collisions at $\sqrt{s} = 1.8$ TeV", *Phys. Rev.* **D71** (2005) 092001, arXiv:hep-ex/0412006.
doi:10.1103/PhysRevD.71.092001.
- [6] CDF Collaboration, "Measurement of correlated $b\bar{b}$ production in $p\bar{p}$ collisions at $\sqrt{s} = 1960$ GeV", *Phys. Rev.* **D77** (2008) 072004, arXiv:0710.1895.
doi:10.1103/PhysRevD.77.072004.
- [7] CMS Collaboration, "The CMS experiment at the CERN LHC", *JINST* **3** (2008) S08004.
doi:10.1088/1748-0221/3/08/S08004.
- [8] G. Zanderighi, "Accurate predictions for heavy quark jets", arXiv:0705.1937.
doi:10.3360/dis.2007.180.
- [9] A. Banfi, G. P. Salam, and G. Zanderighi, "Accurate QCD predictions for heavy-quark jets at the Tevatron and LHC", *JHEP* **07** (2007) 026, arXiv:0704.2999.
doi:10.1088/1126-6708/2007/07/026.
- [10] T. Sjöstrand, S. Mrenna, and P. Z. Skands, "PYTHIA 6.4 Physics and Manual", *JHEP* **05** (2006) 026, arXiv:hep-ph/0603175.
- [11] G. Corcella et al., "HERWIG 6.5: an Event Generator for Hadron Emission Reactions With Interfering Gluons (including supersymmetric processes)", *JHEP* **01** (2001) 010, arXiv:hep-ph/0011363.
- [12] S. Frixione and B. R. Webber, "Matching NLO QCD Computations and Parton Shower Simulations", *JHEP* **06** (2002) 029, arXiv:hep-ph/0204244.
- [13] S. Frixione, P. Nason, and B. R. Webber, "Matching NLO QCD and Parton Showers in Heavy Flavour production", *JHEP* **08** (2003) 007, arXiv:hep-ph/0305252.
- [14] S. Frixione and B. R. Webber, "The MC@NLO 3.4 Event Generator", arXiv:0812.0770.
- [15] M. Cacciari, S. Frixione, M. L. Mangano et al., "Updated Predictions for the Total Production Cross Sections of Top and of Heavier Quark Pairs at the Tevatron and at the LHC", *JHEP* **09** (2008) 127, arXiv:0804.2800.
doi:10.1088/1126-6708/2008/09/127.
- [16] F. Maltoni and T. Stelzer, "MadEvent: Automatic Event Generation with MadGraph", *JHEP* **02** (2003) 027, arXiv:hep-ph/0208156.

- [17] J. Alwall et al., “MadGraph/MadEvent v4: The New Web Generation”, *JHEP* **09** (2007) 028, arXiv:0706.2334.
- [18] H. Jung and G. P. Salam, “Hadronic Final State Predictions from CCFM: The hadron-level Monte Carlo Generator CASCADE”, *Eur. Phys. J.* **C19** (2001) 351, arXiv:hep-ph/0012143. doi:10.1007/s100520100604.
- [19] S. Catani, M. Ciafaloni, and F. Hautmann, “High-energy factorization and small x heavy flavor production”, *Nucl. Phys.* **B366** (1991) 135. doi:10.1016/0550-3213(91)90055-3.
- [20] R. Field, “Studying the Underlying Event at CDF and the LHC”, in *Proceedings of the First International Workshop on Multiple Partonic Interactions at the LHC MPI'08, October 27-31, 2008*, P. Bartalini and L. Fanó, eds. Perugia, Italy, October, 2009. arXiv:1003.4220.
- [21] J. Pumplin et al., “New Generation of Parton Distributions with Uncertainties from Global QCD Analysis”, *JHEP* **07** (2002) 012, arXiv:hep-ph/0201195.
- [22] GEANT4 Collaboration, “GEANT4: A Simulation Toolkit”, *Nucl. Instrum. Meth.* **A506** (2003) 250. doi:10.1016/S0168-9002(03)01368-8.
- [23] J. Alwall, S. de Visscher, and F. Maltoni, “QCD Radiation in the Production of Heavy Colored Particles at the LHC”, *JHEP* **02** (2009) 017, arXiv:0810.5350. doi:10.1088/1126-6708/2009/02/017.
- [24] H. Jung et al., “The CCFM Monte Carlo generator CASCADE 2.2.0”, *Eur. Phys. J.* **C70** (2010) 1237, arXiv:1008.0152. doi:10.1140/epjc/s10052-010-1507-z.
- [25] M. Deak, F. Hautmann, H. Jung et al., “Forward Jet Production at the Large Hadron Collider”, *JHEP* **09** (2009) 121.
- [26] M. Cacciari, G. P. Salam, and G. Soyez, “The anti- k_t Jet Clustering Algorithm”, *JHEP* **04** (2008) 063, arXiv:0802.1189. doi:10.1088/1126-6708/2008/04/063.
- [27] CMS Collaboration, “Tracking and Primary Vertex Results in First 7 TeV Collisions”, *CMS-Note CERN-CMS-PAS-TRK-10-005* (2010).
- [28] CMS Collaboration, “CMS Tracking Performance Results from early LHC Operation”, *Eur. Phys. J.* **C70** (2010) 1165, arXiv:1007.1988. doi:10.1140/epjc/s10052-010-1491-3.
- [29] CMS Collaboration, “Commissioning of the Particle-Flow Reconstruction in Minimum-Bias and Jet Events from pp Collisions at 7 TeV”, *CMS Note CERN-CMS-PAS-PFT-10-002* (2010).
- [30] CMS Collaboration, “Jet Energy Corrections Determination at $\sqrt{s} = 7$ TeV”, *CMS Note CERN-CMS-PAS-JME-10-010* (2010).
- [31] CMS Collaboration, “Jet Performance in pp Collisions at $\sqrt{s} = 7$ TeV”, *CMS Note CERN-CMS-PAS-JME-10-003* (2010).
- [32] R. Frühwirth, W. Waltenberger, and P. Vanlaer, “Adaptive Vertex Fitting”, *J. Phys.* **G34** (2007) N343. doi:10.1088/0954-3899/34/12/N01.
- [33] W. Waltenberger, “Adaptive Vertex Reconstruction”, *CMS Note CERN-CMS-NOTE-2008-033* (2008).

- [34] CMS Collaboration, “First Measurement of the Cross Section for Top-Quark Pair Production in Proton-Proton Collisions at $\text{sqrt}(s)=7 \text{ TeV}$ ”, *Phys. Lett.* **B695** (2011) 424, arXiv:1010.5994. doi:10.1016/j.physletb.2010.11.058.
- [35] Atlas Collaboration, “Measurement of the top quark-pair production cross section with ATLAS in pp collisions at $\sqrt{s} = 7 \text{ TeV}$ ”, arXiv:1012.1792.

A The CMS Collaboration

Yerevan Physics Institute, Yerevan, Armenia
V. Khachatryan, A.M. Sirunyan, A. Tumasyan

Institut für Hochenergiephysik der OeAW, Wien, Austria

W. Adam, T. Bergauer, M. Dragicevic, J. Erö, C. Fabjan, M. Friedl, R. Frühwirth, V.M. Ghete, J. Hammer¹, S. Hänsel, C. Hartl, M. Hoch, N. Hörmann, J. Hrubec, M. Jeitler, G. Kasieczka, W. Kiesenhofer, M. Krammer, D. Liko, I. Mikulec, M. Pernicka, H. Rohringer, R. Schöfbeck, J. Strauss, A. Taurok, F. Teischinger, P. Wagner, W. Waltenberger, G. Walzel, E. Widl, C.-E. Wulz

National Centre for Particle and High Energy Physics, Minsk, Belarus

V. Mossolov, N. Shumeiko, J. Suarez Gonzalez

Universiteit Antwerpen, Antwerpen, Belgium

L. Benucci, K. Cerny, E.A. De Wolf, X. Janssen, T. Maes, L. Mucibello, S. Ochesanu, B. Roland, R. Rougny, M. Selvaggi, H. Van Haevermaet, P. Van Mechelen, N. Van Remortel

Vrije Universiteit Brussel, Brussel, Belgium

S. Beauceron, F. Blekman, S. Blyweert, J. D'Hondt, O. Devroede, R. Gonzalez Suarez, A. Kalogeropoulos, J. Maes, M. Maes, S. Tavernier, W. Van Doninck, P. Van Mulders, G.P. Van Onsem, I. Villella

Université Libre de Bruxelles, Bruxelles, Belgium

O. Charaf, B. Clerbaux, G. De Lentdecker, V. Dero, A.P.R. Gay, G.H. Hammad, T. Hreus, P.E. Marage, L. Thomas, C. Vander Velde, P. Vanlaer, J. Wickens

Ghent University, Ghent, Belgium

V. Adler, S. Costantini, M. Grunewald, B. Klein, A. Marinov, J. Mccartin, D. Ryckbosch, F. Thyssen, M. Tytgat, L. Vanelder, P. Verwilligen, S. Walsh, N. Zaganidis

Université Catholique de Louvain, Louvain-la-Neuve, Belgium

S. Basegmez, G. Bruno, J. Caudron, L. Ceard, J. De Favereau De Jeneret, C. Delaere, P. Demin, D. Favart, A. Giannanco, G. Grégoire, J. Hollar, V. Lemaitre, J. Liao, O. Militaru, S. Ovyn, D. Pagano, A. Pin, K. Piotrkowski, N. Schul

Université de Mons, Mons, Belgium

N. Belyi, T. Caebergs, E. Daubie

Centro Brasileiro de Pesquisas Fisicas, Rio de Janeiro, Brazil

G.A. Alves, D. De Jesus Damiao, M.E. Pol, M.H.G. Souza

Universidade do Estado do Rio de Janeiro, Rio de Janeiro, Brazil

W. Carvalho, E.M. Da Costa, C. De Oliveira Martins, S. Fonseca De Souza, L. Mundim, H. Nogima, V. Oguri, W.L. Prado Da Silva, A. Santoro, S.M. Silva Do Amaral, A. Sznajder, F. Torres Da Silva De Araujo

Instituto de Fisica Teorica, Universidade Estadual Paulista, Sao Paulo, Brazil

F.A. Dias, M.A.F. Dias, T.R. Fernandez Perez Tomei, E. M. Gregores², F. Marinho, S.F. Novaes, Sandra S. Padula

Institute for Nuclear Research and Nuclear Energy, Sofia, Bulgaria

N. Darmenov¹, L. Dimitrov, V. Genchev¹, P. Iaydjiev¹, S. Piperov, M. Rodozov, S. Stoykova, G. Sultanov, V. Tcholakov, R. Trayanov, I. Vankov

University of Sofia, Sofia, Bulgaria

M. Dyulendarova, R. Hadjiiska, V. Kozuharov, L. Litov, E. Marinova, M. Mateev, B. Pavlov, P. Petkov

Institute of High Energy Physics, Beijing, China

J.G. Bian, G.M. Chen, H.S. Chen, C.H. Jiang, D. Liang, S. Liang, J. Wang, J. Wang, X. Wang, Z. Wang, M. Xu, M. Yang, J. Zang, Z. Zhang

State Key Lab. of Nucl. Phys. and Tech., Peking University, Beijing, China

Y. Ban, S. Guo, Y. Guo, W. Li, Y. Mao, S.J. Qian, H. Teng, L. Zhang, B. Zhu, W. Zou

Universidad de Los Andes, Bogota, Colombia

A. Cabrera, B. Gomez Moreno, A.A. Ocampo Rios, A.F. Osorio Oliveros, J.C. Sanabria

Technical University of Split, Split, Croatia

N. Godinovic, D. Lelas, K. Lelas, R. Plestina³, D. Polic, I. Puljak

University of Split, Split, Croatia

Z. Antunovic, M. Dzelalija

Institute Rudjer Boskovic, Zagreb, Croatia

V. Brigljevic, S. Duric, K. Kadija, S. Morovic

University of Cyprus, Nicosia, Cyprus

A. Attikis, M. Galanti, J. Mousa, C. Nicolaou, F. Ptochos, P.A. Razis, H. Rykaczewski

Charles University, Prague, Czech Republic

M. Finger, M. Finger Jr.

Academy of Scientific Research and Technology of the Arab Republic of Egypt, Egyptian Network of High Energy Physics, Cairo, Egypt

Y. Assran⁴, M.A. Mahmoud⁵

National Institute of Chemical Physics and Biophysics, Tallinn, Estonia

A. Hektor, M. Kadastik, K. Kannike, M. Müntel, M. Raidal, L. Rebane

Department of Physics, University of Helsinki, Helsinki, Finland

V. Azzolini, P. Eerola

Helsinki Institute of Physics, Helsinki, Finland

S. Czellar, J. Hätkönen, A. Heikkinen, V. Karimäki, R. Kinnunen, J. Klem, M.J. Kortelainen, T. Lampén, K. Lassila-Perini, S. Lehti, T. Lindén, P. Luukka, T. Mäenpää, E. Tuominen, J. Tuominiemi, E. Tuovinen, D. Ungaro, L. Wendland

Lappeenranta University of Technology, Lappeenranta, Finland

K. Banzuzi, A. Korppela, T. Tuuva

Laboratoire d'Annecy-le-Vieux de Physique des Particules, IN2P3-CNRS, Annecy-le-Vieux, France

D. Sillou

DSM/IRFU, CEA/Saclay, Gif-sur-Yvette, France

M. Besancon, S. Choudhury, M. Dejardin, D. Denegri, B. Fabbro, J.L. Faure, F. Ferri, S. Ganjour, F.X. Gentit, A. Givernaud, P. Gras, G. Hamel de Monchenault, P. Jarry, E. Locci, J. Malcles, M. Marionneau, L. Millischer, J. Rander, A. Rosowsky, I. Shreyber, M. Titov, P. Verrecchia

Laboratoire Leprince-Ringuet, Ecole Polytechnique, IN2P3-CNRS, Palaiseau, France

S. Baffioni, F. Beaudette, L. Bianchini, M. Bluj⁶, C. Broutin, P. Busson, C. Charlot, T. Dahms, L. Dobrzynski, R. Granier de Cassagnac, M. Haguenauer, P. Miné, C. Mironov, C. Ochando, P. Paganini, D. Sabes, R. Salerno, Y. Sirois, C. Thiebaut, B. Wyslouch⁷, A. Zabi

Institut Pluridisciplinaire Hubert Curien, Université de Strasbourg, Université de Haute Alsace Mulhouse, CNRS/IN2P3, Strasbourg, France

J.-L. Agram⁸, J. Andrea, A. Besson, D. Bloch, D. Bodin, J.-M. Brom, M. Cardaci, E.C. Chabert, C. Collard, E. Conte⁸, F. Drouhin⁸, C. Ferro, J.-C. Fontaine⁸, D. Gelé, U. Goerlach, S. Greder, P. Juillot, M. Karim⁸, A.-C. Le Bihan, Y. Mikami, P. Van Hove

Centre de Calcul de l’Institut National de Physique Nucléaire et de Physique des Particules (IN2P3), Villeurbanne, France

F. Fassi, D. Mercier

Université de Lyon, Université Claude Bernard Lyon 1, CNRS-IN2P3, Institut de Physique Nucléaire de Lyon, Villeurbanne, France

C. Baty, N. Beaupere, M. Bedjidian, O. Bondu, G. Boudoul, D. Boumediene, H. Brun, N. Chanon, R. Chierici, D. Contardo, P. Depasse, H. El Mamouni, A. Falkiewicz, J. Fay, S. Gascon, B. Ille, T. Kurca, T. Le Grand, M. Lethuillier, L. Mirabito, S. Perries, V. Sordini, S. Tosi, Y. Tschudi, P. Verdier, H. Xiao

E. Andronikashvili Institute of Physics, Academy of Science, Tbilisi, Georgia

L. Megrelidze, V. Roinishvili

Institute of High Energy Physics and Informatization, Tbilisi State University, Tbilisi, Georgia

D. Lomidze

RWTH Aachen University, I. Physikalisches Institut, Aachen, Germany

G. Anagnostou, M. Edelhoff, L. Feld, N. Heracleous, O. Hindrichs, R. Jussen, K. Klein, J. Merz, N. Mohr, A. Ostapchuk, A. Perieanu, F. Raupach, J. Sammet, S. Schael, D. Sprenger, H. Weber, M. Weber, B. Wittmer

RWTH Aachen University, III. Physikalisches Institut A, Aachen, Germany

M. Ata, W. Bender, M. Erdmann, J. Frangenheim, T. Hebbeker, A. Hinzmann, K. Hoepfner, C. Hof, T. Klimkovich, D. Klingebiel, P. Kreuzer, D. Lanske[†], C. Magass, G. Masetti, M. Merschmeyer, A. Meyer, P. Papacz, H. Pieta, H. Reithler, S.A. Schmitz, L. Sonnenschein, J. Steggemann, D. Teyssier

RWTH Aachen University, III. Physikalisches Institut B, Aachen, Germany

M. Bontenackels, M. Davids, M. Duda, G. Flügge, H. Geenen, M. Giffels, W. Haj Ahmad, D. Heydhausen, T. Kress, Y. Kuessel, A. Linn, A. Nowack, L. Perchalla, O. Pooth, J. Rennefeld, P. Sauerland, A. Stahl, M. Thomas, D. Tornier, M.H. Zoeller

Deutsches Elektronen-Synchrotron, Hamburg, Germany

M. Aldaya Martin, W. Behrenhoff, U. Behrens, M. Bergholz⁹, K. Borras, A. Cakir, A. Campbell, E. Castro, D. Dammann, G. Eckerlin, D. Eckstein, A. Flossdorf, G. Flucke, A. Geiser, I. Glushkov, J. Hauk, H. Jung, M. Kasemann, I. Katkov, P. Katsas, C. Kleinwort, H. Kluge, A. Knutsson, D. Krücker, E. Kuznetsova, W. Lange, W. Lohmann⁹, R. Mankel, M. Marienfeld, I.-A. Melzer-Pellmann, A.B. Meyer, J. Mnich, A. Mussgiller, J. Olzem, A. Parenti, A. Raspereza, A. Raval, R. Schmidt⁹, T. Schoerner-Sadenius, N. Sen, M. Stein, J. Tomaszewska, D. Volyansky, R. Walsh, C. Wissing

University of Hamburg, Hamburg, Germany

C. Autermann, S. Bobrovskyi, J. Draeger, H. Enderle, U. Gebbert, K. Kaschube, G. Kaussen, R. Klanner, J. Lange, B. Mura, S. Naumann-Emme, F. Nowak, N. Pietsch, C. Sander, H. Schettler, P. Schleper, M. Schröder, T. Schum, J. Schwandt, A.K. Srivastava, H. Stadie, G. Steinbrück, J. Thomsen, R. Wolf

Institut für Experimentelle Kernphysik, Karlsruhe, Germany

C. Barth, J. Bauer, V. Buege, T. Chwalek, W. De Boer, A. Dierlamm, G. Dirkes, M. Feindt, J. Gruschke, C. Hackstein, F. Hartmann, S.M. Heindl, M. Heinrich, H. Held, K.H. Hoffmann, S. Honc, T. Kuhr, D. Martschei, S. Mueller, Th. Müller, M. Niegel, O. Oberst, A. Oehler, J. Ott, T. Peiffer, D. Piparo, G. Quast, K. Rabbertz, F. Ratnikov, M. Renz, C. Saout, A. Scheurer, P. Schieferdecker, F.-P. Schilling, G. Schott, H.J. Simonis, F.M. Stober, D. Troendle, J. Wagner-Kuhr, M. Zeise, V. Zhukov¹⁰, E.B. Ziebarth

Institute of Nuclear Physics "Demokritos", Aghia Paraskevi, Greece

G. Daskalakis, T. Geralis, S. Kesisoglou, A. Kyriakis, D. Loukas, I. Manolakos, A. Markou, C. Markou, C. Mavrommatis, E. Ntomari, E. Petrakou

University of Athens, Athens, Greece

L. Gouskos, T.J. Mertzimekis, A. Panagiotou

University of Ioánnina, Ioánnina, Greece

I. Evangelou, C. Foudas, P. Kokkas, N. Manthos, I. Papadopoulos, V. Patras, F.A. Triantis

KFKI Research Institute for Particle and Nuclear Physics, Budapest, Hungary

A. Aranyi, G. Bencze, L. Boldizsar, G. Debreczeni, C. Hajdu¹, D. Horvath¹¹, A. Kapusi, K. Krajczar¹², A. Laszlo, F. Sikler, G. Vesztergombi¹²

Institute of Nuclear Research ATOMKI, Debrecen, Hungary

N. Beni, J. Molnar, J. Palinkas, Z. Szillasi, V. Veszpremi

University of Debrecen, Debrecen, Hungary

P. Raics, Z.L. Trocsanyi, B. Ujvari

Panjab University, Chandigarh, India

S. Bansal, S.B. Beri, V. Bhatnagar, N. Dhingra, R. Gupta, M. Jindal, M. Kaur, J.M. Kohli, M.Z. Mehta, N. Nishu, L.K. Saini, A. Sharma, A.P. Singh, J.B. Singh, S.P. Singh

University of Delhi, Delhi, India

S. Ahuja, S. Bhattacharya, B.C. Choudhary, P. Gupta, S. Jain, S. Jain, A. Kumar, R.K. Shivpuri

Bhabha Atomic Research Centre, Mumbai, India

R.K. Choudhury, D. Dutta, S. Kailas, S.K. Kataria, A.K. Mohanty¹, L.M. Pant, P. Shukla

Tata Institute of Fundamental Research - EHEP, Mumbai, India

T. Aziz, M. Guchait¹³, A. Gurtu, M. Maity¹⁴, D. Majumder, G. Majumder, K. Mazumdar, G.B. Mohanty, A. Saha, K. Sudhakar, N. Wickramage

Tata Institute of Fundamental Research - HECR, Mumbai, India

S. Banerjee, S. Dugad, N.K. Mondal

Institute for Research and Fundamental Sciences (IPM), Tehran, Iran

H. Arfaei, H. Bakhshiansohi, S.M. Etesami, A. Fahim, M. Hashemi, A. Jafari, M. Khakzad, A. Mohammadi, M. Mohammadi Najafabadi, S. Paktnat Mehdiabadi, B. Safarzadeh, M. Zeinali

INFN Sezione di Bari ^a, Università di Bari ^b, Politecnico di Bari ^c, Bari, Italy

M. Abbrescia^{a,b}, L. Barbone^{a,b}, C. Calabria^{a,b}, A. Colaleo^a, D. Creanza^{a,c}, N. De Filippis^{a,c}, M. De Palma^{a,b}, A. Dimitrov^a, L. Fiore^a, G. Iaselli^{a,c}, L. Lusito^{a,b,1}, G. Maggi^{a,c}, M. Maggi^a, N. Manna^{a,b}, B. Marangelli^{a,b}, S. My^{a,c}, S. Nuzzo^{a,b}, N. Pacifico^{a,b}, G.A. Pierro^a, A. Pompili^{a,b}, G. Pugliese^{a,c}, F. Romano^{a,c}, G. Roselli^{a,b}, G. Selvaggi^{a,b}, L. Silvestris^a, R. Trentadue^a, S. Tupputi^{a,b}, G. Zito^a

INFN Sezione di Bologna ^a, Università di Bologna ^b, Bologna, Italy

G. Abbiendi^a, A.C. Benvenuti^a, D. Bonacorsi^a, S. Braibant-Giacomelli^{a,b}, L. Brigliadori^a, P. Capiluppi^{a,b}, A. Castro^{a,b}, F.R. Cavallo^a, M. Cuffiani^{a,b}, G.M. Dallavalle^a, F. Fabbri^a, A. Fanfani^{a,b}, D. Fasanella^a, P. Giacomelli^a, M. Giunta^a, C. Grandi^a, S. Marcellini^a, M. Meneghelli^{a,b}, A. Montanari^a, F.L. Navarria^{a,b}, F. Odorici^a, A. Perrotta^a, F. Primavera^a, A.M. Rossi^{a,b}, T. Rovelli^{a,b}, G. Siroli^{a,b}, R. Travaglini^{a,b}

INFN Sezione di Catania ^a, Università di Catania ^b, Catania, Italy

S. Albergo^{a,b}, G. Cappello^{a,b}, M. Chiorboli^{a,b,1}, S. Costa^{a,b}, A. Tricomi^{a,b}, C. Tuve^a

INFN Sezione di Firenze ^a, Università di Firenze ^b, Firenze, Italy

G. Barbagli^a, V. Ciulli^{a,b}, C. Civinini^a, R. D'Alessandro^{a,b}, E. Focardi^{a,b}, S. Frosali^{a,b}, E. Gallo^a, S. Gonzi^{a,b}, P. Lenzi^{a,b}, M. Meschini^a, S. Paoletti^a, G. Sguazzoni^a, A. Tropiano^{a,1}

INFN Laboratori Nazionali di Frascati, Frascati, Italy

L. Benussi, S. Bianco, S. Colafranceschi¹⁵, F. Fabbri, D. Piccolo

INFN Sezione di Genova, Genova, Italy

P. Fabbricatore, R. Musenich

INFN Sezione di Milano-Biccoca ^a, Università di Milano-Bicocca ^b, Milano, Italy

A. Benaglia^{a,b}, F. De Guio^{a,b,1}, L. Di Matteo^{a,b}, A. Ghezzi^{a,b,1}, M. Malberti^{a,b}, S. Malvezzi^a, A. Martelli^{a,b}, A. Massironi^{a,b}, D. Menasce^a, L. Moroni^a, M. Paganoni^{a,b}, D. Pedrini^a, S. Ragazzi^{a,b}, N. Redaelli^a, S. Sala^a, T. Tabarelli de Fatis^{a,b}, V. Tancini^{a,b}

INFN Sezione di Napoli ^a, Università di Napoli "Federico II" ^b, Napoli, Italy

S. Buontempo^a, C.A. Carrillo Montoya^a, A. Cimmino^{a,b}, A. De Cosa^{a,b}, M. De Gruttola^{a,b}, F. Fabozzi^{a,16}, A.O.M. Iorio^a, L. Lista^a, M. Merola^{a,b}, P. Noli^{a,b}, P. Paolucci^a

INFN Sezione di Padova ^a, Università di Padova ^b, Università di Trento (Trento) ^c, Padova, Italy

P. Azzi^a, N. Bacchetta^a, P. Bellan^{a,b}, A. Branca^a, R. Carlin^{a,b}, P. Checchia^a, M. De Mattia^{a,b}, T. Dorigo^a, U. Dosselli^a, F. Gasparini^{a,b}, U. Gasparini^{a,b}, P. Giubilato^{a,b}, A. Gresele^{a,c}, A. Kaminskiy^{a,b}, S. Lacaprara^{a,17}, I. Lazzizzera^{a,c}, M. Margoni^{a,b}, M. Mazzucato^a, A.T. Meneguzzo^{a,b}, M. Nespolo^{a,1}, M. Passaseo^a, L. Perrozzi^{a,1}, N. Pozzobon^{a,b}, P. Ronchese^{a,b}, F. Simonetto^{a,b}, E. Torassa^a, M. Tosi^{a,b}, A. Triassi^a, S. Vanini^{a,b}, G. Zumerle^{a,b}

INFN Sezione di Pavia ^a, Università di Pavia ^b, Pavia, Italy

U. Berzano^a, C. Riccardi^{a,b}, P. Torre^{a,b}, P. Vitulo^{a,b}

INFN Sezione di Perugia ^a, Università di Perugia ^b, Perugia, Italy

M. Biasini^{a,b}, G.M. Bilei^a, B. Caponeri^{a,b}, L. Fanò^{a,b}, P. Lariccia^{a,b}, A. Lucaroni^{a,b,1}, G. Mantovani^{a,b}, M. Menichelli^a, A. Nappi^{a,b}, A. Santocchia^{a,b}, L. Servoli^a, S. Taroni^{a,b}, M. Valdata^{a,b}, R. Volpe^{a,b,1}

INFN Sezione di Pisa ^a, Università di Pisa ^b, Scuola Normale Superiore di Pisa ^c, Pisa, Italy

P. Azzurri^{a,c}, G. Bagliesi^a, J. Bernardini^{a,b}, T. Boccali^{a,1}, G. Broccolo^{a,c}, R. Castaldi^a, R.T. D'Agnolo^{a,c}, R. Dell'Orso^a, F. Fiori^{a,b}, L. Foà^{a,c}, A. Giassi^a, A. Kraan^a, F. Ligabue^{a,c},

T. Lomtadze^a, L. Martini^{a,18}, A. Messineo^{a,b}, F. Palla^a, F. Palmonari^a, S. Sarkar^{a,c}, G. Segneri^a, A.T. Serban^a, P. Spagnolo^a, R. Tenchini^a, G. Tonelli^{a,b,1}, A. Venturi^{a,1}, P.G. Verdini^a

INFN Sezione di Roma ^a, Università di Roma "La Sapienza" ^b, Roma, Italy

L. Barone^{a,b}, F. Cavallari^a, D. Del Re^{a,b}, E. Di Marco^{a,b}, M. Diemoz^a, D. Franci^{a,b}, M. Grassi^a, E. Longo^{a,b}, S. Nourbakhsh^a, G. Organtini^{a,b}, A. Palma^{a,b}, F. Pandolfi^{a,b,1}, R. Paramatti^a, S. Rahatlou^{a,b}

INFN Sezione di Torino ^a, Università di Torino ^b, Università del Piemonte Orientale (Novara) ^c, Torino, Italy

N. Amapane^{a,b}, R. Arcidiacono^{a,c}, S. Argiro^{a,b}, M. Arneodo^{a,c}, C. Biino^a, C. Botta^{a,b,1}, N. Cartiglia^a, R. Castello^{a,b}, M. Costa^{a,b}, N. Demaria^a, A. Graziano^{a,b,1}, C. Mariotti^a, M. Marone^{a,b}, S. Maselli^a, E. Migliore^{a,b}, G. Mila^{a,b}, V. Monaco^{a,b}, M. Musich^{a,b}, M.M. Obertino^{a,c}, N. Pastrone^a, M. Pelliccioni^{a,b,1}, A. Romero^{a,b}, M. Ruspa^{a,c}, R. Sacchi^{a,b}, V. Sola^{a,b}, A. Solano^{a,b}, A. Staiano^a, D. Trocino^{a,b}, A. Vilela Pereira^{a,b,1}

INFN Sezione di Trieste ^a, Università di Trieste ^b, Trieste, Italy

S. Belforte^a, F. Cossutti^a, G. Della Ricca^{a,b}, B. Gobbo^a, D. Montanino^{a,b}, A. Penzo^a

Kangwon National University, Chunchon, Korea

S.G. Heo

Kyungpook National University, Daegu, Korea

S. Chang, J. Chung, D.H. Kim, G.N. Kim, J.E. Kim, D.J. Kong, H. Park, D. Son, D.C. Son

Chonnam National University, Institute for Universe and Elementary Particles, Kwangju, Korea

Zero Kim, J.Y. Kim, S. Song

Korea University, Seoul, Korea

S. Choi, B. Hong, M. Jo, H. Kim, J.H. Kim, T.J. Kim, K.S. Lee, D.H. Moon, S.K. Park, H.B. Rhee, E. Seo, S. Shin, K.S. Sim

University of Seoul, Seoul, Korea

M. Choi, S. Kang, H. Kim, C. Park, I.C. Park, S. Park, G. Ryu

Sungkyunkwan University, Suwon, Korea

Y. Choi, Y.K. Choi, J. Goh, J. Lee, S. Lee, H. Seo, I. Yu

Vilnius University, Vilnius, Lithuania

M.J. Bilinskas, I. Grigelionis, M. Janulis, D. Martisiute, P. Petrov, T. Sabonis

Centro de Investigacion y de Estudios Avanzados del IPN, Mexico City, Mexico

H. Castilla-Valdez, E. De La Cruz-Burelo, R. Lopez-Fernandez, A. Sánchez-Hernández, L.M. Villasenor-Cendejas

Universidad Iberoamericana, Mexico City, Mexico

S. Carrillo Moreno, F. Vazquez Valencia

Benemerita Universidad Autonoma de Puebla, Puebla, Mexico

H.A. Salazar Ibarguen

Universidad Autónoma de San Luis Potosí, San Luis Potosí, Mexico

E. Casimiro Linares, A. Morelos Pineda, M.A. Reyes-Santos

University of Auckland, Auckland, New Zealand

P. Allfrey, D. Korfcheck

University of Canterbury, Christchurch, New Zealand
P.H. Butler, R. Doesburg, H. Silverwood

National Centre for Physics, Quaid-I-Azam University, Islamabad, Pakistan
M. Ahmad, I. Ahmed, M.I. Asghar, H.R. Hoorani, W.A. Khan, T. Khurshid, S. Qazi

Institute of Experimental Physics, Faculty of Physics, University of Warsaw, Warsaw, Poland
M. Cwiok, W. Dominik, K. Doroba, A. Kalinowski, M. Konecki, J. Krolikowski

Soltan Institute for Nuclear Studies, Warsaw, Poland
T. Frueboes, R. Gokieli, M. Górski, M. Kazana, K. Nawrocki, K. Romanowska-Rybinska, M. Szleper, G. Wrochna, P. Zalewski

Laboratório de Instrumentação e Física Experimental de Partículas, Lisboa, Portugal
N. Almeida, A. David, P. Faccioli, P.G. Ferreira Parracho, M. Gallinaro, P. Martins, P. Musella, A. Nayak, P.Q. Ribeiro, J. Seixas, P. Silva, J. Varela, H.K. Wöhri

Joint Institute for Nuclear Research, Dubna, Russia
I. Belotelov, P. Bunin, I. Golutvin, A. Kamenev, V. Karjavin, G. Kozlov, A. Lanev, P. Moisenz, V. Palichik, V. Perelygin, S. Shmatov, V. Smirnov, A. Volodko, A. Zarubin

Petersburg Nuclear Physics Institute, Gatchina (St Petersburg), Russia
N. Bondar, V. Golovtsov, Y. Ivanov, V. Kim, P. Levchenko, V. Murzin, V. Oreshkin, I. Smirnov, V. Sulimov, L. Uvarov, S. Vavilov, A. Vorobyev

Institute for Nuclear Research, Moscow, Russia
Yu. Andreev, S. Glinenko, N. Golubev, M. Kirsanov, N. Krasnikov, V. Matveev, A. Pashenkov, A. Toropin, S. Troitsky

Institute for Theoretical and Experimental Physics, Moscow, Russia
V. Epshteyn, V. Gavrilov, V. Kaftanov[†], M. Kossov¹, A. Krokhotin, N. Lychkovskaya, G. Safronov, S. Semenov, V. Stolin, E. Vlasov, A. Zhokin

Moscow State University, Moscow, Russia
E. Boos, M. Dubinin¹⁹, L. Dudko, A. Ershov, A. Gribushin, O. Kodolova, I. Loktin, S. Obraztsov, S. Petrushanko, L. Sarycheva, V. Savrin, A. Snigirev

P.N. Lebedev Physical Institute, Moscow, Russia
V. Andreev, M. Azarkin, I. Dremin, M. Kirakosyan, S.V. Rusakov, A. Vinogradov

State Research Center of Russian Federation, Institute for High Energy Physics, Protvino, Russia
I. Azhgirey, S. Bitiukov, V. Grishin¹, V. Kachanov, D. Konstantinov, A. Korablev, V. Krychkine, V. Petrov, R. Ryutin, S. Slabospitsky, A. Sobol, L. Tourtchanovitch, S. Troshin, N. Tyurin, A. Uzunian, A. Volkov

University of Belgrade, Faculty of Physics and Vinca Institute of Nuclear Sciences, Belgrade, Serbia
P. Adzic²⁰, M. Djordjevic, D. Krpic²⁰, J. Milosevic

Centro de Investigaciones Energéticas Medioambientales y Tecnológicas (CIEMAT), Madrid, Spain
M. Aguilar-Benitez, J. Alcaraz Maestre, P. Arce, C. Battilana, E. Calvo, M. Cepeda, M. Cerrada, N. Colino, B. De La Cruz, C. Diez Pardos, D. Domínguez Vázquez, C. Fernandez Bedoya, J.P. Fernández Ramos, A. Ferrando, J. Flix, M.C. Fouz, P. Garcia-Abia, O. Gonzalez Lopez,

S. Goy Lopez, J.M. Hernandez, M.I. Josa, G. Merino, J. Puerta Pelayo, I. Redondo, L. Romero, J. Santaolalla, C. Willmott

Universidad Autónoma de Madrid, Madrid, Spain

C. Albajar, G. Codispoti, J.F. de Trocóniz

Universidad de Oviedo, Oviedo, Spain

J. Cuevas, J. Fernandez Menendez, S. Folgueras, I. Gonzalez Caballero, L. Lloret Iglesias, J.M. Vizan Garcia

Instituto de Física de Cantabria (IFCA), CSIC-Universidad de Cantabria, Santander, Spain

J.A. Brochero Cifuentes, I.J. Cabrillo, A. Calderon, M. Chamizo Llatas, S.H. Chuang, J. Duarte Campderros, M. Felcini²¹, M. Fernandez, G. Gomez, J. Gonzalez Sanchez, C. Jorda, P. Lobelle Pardo, A. Lopez Virto, J. Marco, R. Marco, C. Martinez Rivero, F. Matorras, F.J. Munoz Sanchez, J. Piedra Gomez²², T. Rodrigo, A. Ruiz-Jimeno, L. Scodellaro, M. Sobron Sanudo, I. Vila, R. Vilar Cortabitarte

CERN, European Organization for Nuclear Research, Geneva, Switzerland

D. Abbaneo, E. Auffray, G. Auzinger, P. Baillon, A.H. Ball, D. Barney, A.J. Bell²³, D. Benedetti, C. Bernet³, W. Bialas, P. Bloch, A. Bocci, S. Bolognesi, H. Breuker, G. Brona, K. Bunkowski, T. Camporesi, E. Cano, G. Cerminara, T. Christiansen, J.A. Coarasa Perez, B. Curé, D. D'Enterria, A. De Roeck, S. Di Guida, F. Duarte Ramos, A. Elliott-Peisert, B. Frisch, W. Funk, A. Gaddi, S. Gennai, G. Georgiou, H. Gerwig, D. Gigi, K. Gill, D. Giordano, F. Glege, R. Gomez-Reino Garrido, M. Gouzevitch, P. Govoni, S. Gowdy, L. Guiducci, M. Hansen, J. Harvey, J. Hegeman, B. Hegner, C. Henderson, G. Hesketh, H.F. Hoffmann, A. Honma, V. Innocente, P. Janot, K. Kaadze, E. Karavakis, P. Lecoq, C. Lourenço, A. Macpherson, T. Mäki, L. Malgeri, M. Mannelli, L. Masetti, F. Meijers, S. Mersi, E. Meschi, R. Moser, M.U. Mozer, M. Mulders, E. Nesvold¹, M. Nguyen, T. Orimoto, L. Orsini, E. Perez, A. Petrilli, A. Pfeiffer, M. Pierini, M. Pimiä, G. Polese, A. Racz, J. Rodrigues Antunes, G. Rolandi²⁴, T. Rommerskirchen, C. Rovelli²⁵, M. Rovere, H. Sakulin, C. Schäfer, C. Schwick, I. Segoni, A. Sharma, P. Siegrist, M. Simon, P. Sphicas²⁶, D. Spiga, M. Spiropulu¹⁹, F. Stöckli, M. Stoye, P. Tropea, A. Tsirou, A. Tsyganov, G.I. Veres¹², P. Vichoudis, M. Voutilainen, W.D. Zeuner

Paul Scherrer Institut, Villigen, Switzerland

W. Bertl, K. Deiters, W. Erdmann, K. Gabathuler, R. Horisberger, Q. Ingram, H.C. Kaestli, S. König, D. Kotlinski, U. Langenegger, F. Meier, D. Renker, T. Rohe, J. Sibille²⁷, A. Starodumov²⁸

Institute for Particle Physics, ETH Zurich, Zurich, Switzerland

P. Bortignon, L. Caminada²⁹, Z. Chen, S. Cittolin, G. Dissertori, M. Dittmar, J. Eugster, K. Freudenreich, C. Grab, A. Hervé, W. Hintz, P. Lecomte, W. Lustermann, C. Marchica²⁹, P. Martinez Ruiz del Arbol, P. Meridiani, P. Milenovic³⁰, F. Moortgat, P. Nef, F. Nessi-Tedaldi, L. Pape, F. Pauss, T. Punz, A. Rizzi, F.J. Ronga, M. Rossini, L. Sala, A.K. Sanchez, M.-C. Sawley, B. Stieger, L. Tauscher[†], A. Thea, K. Theofilatos, D. Treille, C. Urscheler, R. Wallny, M. Weber, L. Wehrli, J. Weng

Universität Zürich, Zurich, Switzerland

E. Aguiló, C. Amsler, V. Chiochia, S. De Visscher, C. Favaro, M. Ivova Rikova, B. Millan Mejias, P. Otiougova, C. Regenfus, P. Robmann, A. Schmidt, H. Snoek

National Central University, Chung-Li, Taiwan

Y.H. Chang, K.H. Chen, W.T. Chen, S. Dutta, A. Go, C.M. Kuo, S.W. Li, W. Lin, M.H. Liu, Z.K. Liu, Y.J. Lu, D. Mekterovic, J.H. Wu, S.S. Yu

National Taiwan University (NTU), Taipei, Taiwan

P. Bartalini, P. Chang, Y.H. Chang, Y.W. Chang, Y. Chao, K.F. Chen, W.-S. Hou, Y. Hsiung, K.Y. Kao, Y.J. Lei, R.-S. Lu, J.G. Shiu, Y.M. Tzeng, M. Wang

Cukurova University, Adana, Turkey

A. Adiguzel, M.N. Bakirci³¹, S. Cerci³², Z. Demir, C. Dozen, I. Dumanoglu, E. Eskut, S. Girgis, G. Gokbulut, Y. Guler, E. Gurpinar, I. Hos, E.E. Kangal, T. Karaman, A. Kayis Topaksu, A. Nart, G. Onengut, K. Ozdemir, S. Ozturk, A. Polatoz, K. Sogut³³, B. Tali, H. Topakli³¹, D. Uzun, L.N. Vergili, M. Vergili, C. Zorbilmez

Middle East Technical University, Physics Department, Ankara, Turkey

I.V. Akin, T. Aliev, S. Bilmis, M. Deniz, H. Gamsizkan, A.M. Guler, K. Ocalan, A. Ozpineci, M. Serin, R. Sever, U.E. Surat, E. Yildirim, M. Zeyrek

Bogazici University, Istanbul, Turkey

M. Deliomeroglu, D. Demir³⁴, E. Glmez, A. Halu, B. Isildak, M. Kaya³⁵, O. Kaya³⁵, S. Ozkorucuklu³⁶, N. Sonmez³⁷

National Scientific Center, Kharkov Institute of Physics and Technology, Kharkov, Ukraine

L. Levchuk

University of Bristol, Bristol, United Kingdom

P. Bell, F. Bostock, J.J. Brooke, T.L. Cheng, E. Clement, D. Cussans, R. Frazier, J. Goldstein, M. Grimes, M. Hansen, D. Hartley, G.P. Heath, H.F. Heath, B. Huckvale, J. Jackson, L. Kreczko, S. Metson, D.M. Newbold³⁸, K. Nirunpong, A. Poll, S. Senkin, V.J. Smith, S. Ward

Rutherford Appleton Laboratory, Didcot, United Kingdom

L. Basso, K.W. Bell, A. Belyaev, C. Brew, R.M. Brown, B. Camanzi, D.J.A. Cockerill, J.A. Coughlan, K. Harder, S. Harper, B.W. Kennedy, E. Olaiya, D. Petyt, B.C. Radburn-Smith, C.H. Shepherd-Themistocleous, I.R. Tomalin, W.J. Womersley, S.D. Worm

Imperial College, London, United Kingdom

R. Bainbridge, G. Ball, J. Ballin, R. Beuselinck, O. Buchmuller, D. Colling, N. Cripps, M. Cutajar, G. Davies, M. Della Negra, J. Fulcher, D. Futyan, A. Guneratne Bryer, G. Hall, Z. Hatherell, J. Hays, G. Iles, G. Karapostoli, L. Lyons, A.-M. Magnan, J. Marrouche, R. Nandi, J. Nash, A. Nikitenko²⁸, A. Papageorgiou, M. Pesaresi, K. Petridis, M. Pioppi³⁹, D.M. Raymond, N. Rompotis, A. Rose, M.J. Ryan, C. Seez, P. Sharp, A. Sparrow, A. Tapper, S. Tourneur, M. Vazquez Acosta, T. Virdee, S. Wakefield, D. Wardrope, T. Whyntie

Brunel University, Uxbridge, United Kingdom

M. Barrett, M. Chadwick, J.E. Cole, P.R. Hobson, A. Khan, P. Kyberd, D. Leslie, W. Martin, I.D. Reid, L. Teodorescu

Baylor University, Waco, USA

K. Hatakeyama

Boston University, Boston, USA

T. Bose, E. Carrera Jarrin, C. Fantasia, A. Heister, J. St. John, P. Lawson, D. Lazic, J. Rohlf, D. Sperka, L. Sulak

Brown University, Providence, USA

A. Avetisyan, S. Bhattacharya, J.P. Chou, D. Cutts, A. Ferapontov, U. Heintz, S. Jabeen, G. Kukartsev, G. Landsberg, M. Narain, D. Nguyen, M. Segala, T. Speer, K.V. Tsang

University of California, Davis, Davis, USA

M.A. Borgia, R. Breedon, M. Calderon De La Barca Sanchez, D. Cebra, S. Chauhan, M. Chertok, J. Conway, P.T. Cox, J. Dolen, R. Erbacher, E. Friis, W. Ko, A. Kopecky, R. Lander, H. Liu, S. Maruyama, T. Miceli, M. Nikolic, D. Pellett, J. Robles, S. Salur, T. Schwarz, M. Searle, J. Smith, M. Squires, M. Tripathi, R. Vasquez Sierra, C. Veelken

University of California, Los Angeles, Los Angeles, USA

V. Andreev, K. Arisaka, D. Cline, R. Cousins, A. Deisher, J. Duris, S. Erhan, C. Farrell, J. Hauser, M. Ignatenko, C. Jarvis, C. Plager, G. Rakness, P. Schlein[†], J. Tucker, V. Valuev

University of California, Riverside, Riverside, USA

J. Babb, R. Clare, J. Ellison, J.W. Gary, F. Giordano, G. Hanson, G.Y. Jeng, S.C. Kao, F. Liu, H. Liu, A. Luthra, H. Nguyen, B.C. Shen[†], R. Stringer, J. Sturdy, S. Sumowidagdo, R. Wilken, S. Wimpenny

University of California, San Diego, La Jolla, USA

W. Andrews, J.G. Branson, G.B. Cerati, E. Dusinberre, D. Evans, F. Golf, A. Holzner, R. Kelley, M. Lebourgeois, J. Letts, B. Mangano, J. Muelmenstaedt, S. Padhi, C. Palmer, G. Petrucciani, H. Pi, M. Pieri, R. Ranieri, M. Sani, V. Sharma¹, S. Simon, Y. Tu, A. Vartak, F. Würthwein, A. Yagil

University of California, Santa Barbara, Santa Barbara, USA

D. Barge, R. Bellan, C. Campagnari, M. D'Alfonso, T. Danielson, K. Flowers, P. Geffert, J. Incandela, C. Justus, P. Kalavase, S.A. Koay, D. Kovalskyi, V. Krutelyov, S. Lowette, N. Mccoll, V. Pavlunin, F. Rebassoo, J. Ribnik, J. Richman, R. Rossin, D. Stuart, W. To, J.R. Vlimant

California Institute of Technology, Pasadena, USA

A. Bornheim, J. Bunn, Y. Chen, M. Gataullin, D. Kcira, V. Litvine, Y. Ma, A. Mott, H.B. Newman, C. Rogan, V. Timciuc, P. Traczyk, J. Veverka, R. Wilkinson, Y. Yang, R.Y. Zhu

Carnegie Mellon University, Pittsburgh, USA

B. Akgun, R. Carroll, T. Ferguson, Y. Iiyama, D.W. Jang, S.Y. Jun, Y.F. Liu, M. Paulini, J. Russ, N. Terentyev, H. Vogel, I. Vorobiev

University of Colorado at Boulder, Boulder, USA

J.P. Cumalat, M.E. Dinardo, B.R. Drell, C.J. Edelmaier, W.T. Ford, A. Gaz, B. Heyburn, E. Luiggi Lopez, U. Nauenberg, J.G. Smith, K. Stenson, K.A. Ulmer, S.R. Wagner, S.L. Zang

Cornell University, Ithaca, USA

L. Agostino, J. Alexander, A. Chatterjee, S. Das, N. Eggert, L.J. Fields, L.K. Gibbons, B. Heltsley, W. Hopkins, A. Khukhunaishvili, B. Kreis, V. Kuznetsov, G. Nicolas Kaufman, J.R. Patterson, D. Puigh, D. Riley, A. Ryd, X. Shi, W. Sun, W.D. Teo, J. Thom, J. Thompson, J. Vaughan, Y. Weng, L. Winstrom, P. Wittich

Fairfield University, Fairfield, USA

A. Biselli, G. Cirino, D. Winn

Fermi National Accelerator Laboratory, Batavia, USA

S. Abdullin, M. Albrow, J. Anderson, G. Apolinari, M. Atac, J.A. Bakken, S. Banerjee, L.A.T. Bauerick, A. Beretvas, J. Berryhill, P.C. Bhat, I. Bloch, F. Borcherding, K. Burkett, J.N. Butler, V. Chetluru, H.W.K. Cheung, F. Chlebana, S. Cihangir, M. Demarteau, D.P. Eartly, V.D. Elvira, S. Esen, I. Fisk, J. Freeman, Y. Gao, E. Gottschalk, D. Green, K. Gunthot, O. Gutsche, A. Hahn, J. Hanlon, R.M. Harris, J. Hirschauer, B. Hooberman, E. James, H. Jensen, M. Johnson, U. Joshi, R. Khatiwada, B. Kilminster, B. Klima, K. Kousouris, S. Kunori, S. Kwan,

C. Leonidopoulos, P. Limon, R. Lipton, J. Lykken, K. Maeshima, J.M. Marraffino, D. Mason, P. McBride, T. McCauley, T. Miao, K. Mishra, S. Mrenna, Y. Musienko⁴⁰, C. Newman-Holmes, V. O'Dell, S. Popescu⁴¹, R. Pordes, O. Prokofyev, N. Saoulidou, E. Sexton-Kennedy, S. Sharma, A. Soha, W.J. Spalding, L. Spiegel, P. Tan, L. Taylor, S. Tkaczyk, L. Uplegger, E.W. Vaandering, R. Vidal, J. Whitmore, W. Wu, F. Yang, F. Yumiceva, J.C. Yun

University of Florida, Gainesville, USA

D. Acosta, P. Avery, D. Bourilkov, M. Chen, G.P. Di Giovanni, D. Dobur, A. Drozdetskiy, R.D. Field, M. Fisher, Y. Fu, I.K. Furic, J. Gartner, S. Goldberg, B. Kim, S. Klimenko, J. Konigsberg, A. Korytov, A. Kropivnitskaya, T. Kypreos, K. Matchev, G. Mitselmakher, L. Muniz, Y. Pakhotin, C. Prescott, R. Remington, M. Schmitt, B. Scurlock, P. Sellers, N. Skhirtladze, D. Wang, J. Yelton, M. Zakaria

Florida International University, Miami, USA

C. Ceron, V. Gaultney, L. Kramer, L.M. Lebolo, S. Linn, P. Markowitz, G. Martinez, J.L. Rodriguez

Florida State University, Tallahassee, USA

T. Adams, A. Askew, D. Bandurin, J. Bochenek, J. Chen, B. Diamond, S.V. Gleyzer, J. Haas, S. Hagopian, V. Hagopian, M. Jenkins, K.F. Johnson, H. Prosper, L. Quertenmont, S. Sekmen, V. Veeraraghavan

Florida Institute of Technology, Melbourne, USA

M.M. Baarmand, B. Dorney, S. Guragain, M. Hohlmann, H. Kalakhety, R. Ralich, I. Vodopiyanov

University of Illinois at Chicago (UIC), Chicago, USA

M.R. Adams, I.M. Anghel, L. Apanasevich, Y. Bai, V.E. Bazterra, R.R. Betts, J. Callner, R. Cavanaugh, C. Dragoiu, E.J. Garcia-Solis, L. Gauthier, C.E. Gerber, D.J. Hofman, S. Khalatyan, F. Lacroix, M. Malek, C. O'Brien, C. Silvestre, A. Smoron, D. Strom, N. Varelas

The University of Iowa, Iowa City, USA

U. Akgun, E.A. Albayrak, B. Bilki, K. Cankocak⁴², W. Clarida, F. Duru, C.K. Lae, E. McCliment, J.-P. Merlo, H. Mermerkaya, A. Mestvirishvili, A. Moeller, J. Nachtman, C.R. Newsom, E. Norbeck, J. Olson, Y. Onel, F. Ozok, S. Sen, J. Wetzel, T. Yetkin, K. Yi

Johns Hopkins University, Baltimore, USA

B.A. Barnett, B. Blumenfeld, A. Bonato, C. Eskew, D. Fehling, G. Giurgiu, A.V. Gritsan, Z.J. Guo, G. Hu, P. Maksimovic, S. Rappoccio, M. Swartz, N.V. Tran, A. Whitbeck

The University of Kansas, Lawrence, USA

P. Baringer, A. Bean, G. Benelli, O. Grachov, M. Murray, D. Noonan, V. Radicci, S. Sanders, J.S. Wood, V. Zhukova

Kansas State University, Manhattan, USA

T. Bolton, I. Chakaberia, A. Ivanov, M. Makouski, Y. Maravin, S. Shrestha, I. Svintradze, Z. Wan

Lawrence Livermore National Laboratory, Livermore, USA

J. Gronberg, D. Lange, D. Wright

University of Maryland, College Park, USA

A. Baden, M. Boutemeur, S.C. Eno, D. Ferencek, J.A. Gomez, N.J. Hadley, R.G. Kellogg, M. Kirn, Y. Lu, A.C. Mignerey, K. Rossato, P. Rumerio, F. Santanastasio, A. Skuja, J. Temple, M.B. Tonjes, S.C. Tonwar, E. Twedt

Massachusetts Institute of Technology, Cambridge, USA

B. Alver, G. Bauer, J. Bendavid, W. Busza, E. Butz, I.A. Cali, M. Chan, V. Dutta, P. Everaerts, G. Gomez Ceballos, M. Goncharov, K.A. Hahn, P. Harris, Y. Kim, M. Klute, Y.-J. Lee, W. Li, C. Loizides, P.D. Luckey, T. Ma, S. Nahn, C. Paus, D. Ralph, C. Roland, G. Roland, M. Rudolph, G.S.F. Stephans, K. Sumorok, K. Sung, E.A. Wenger, S. Xie, M. Yang, Y. Yilmaz, A.S. Yoon, M. Zanetti

University of Minnesota, Minneapolis, USA

P. Cole, S.I. Cooper, P. Cushman, B. Dahmes, A. De Benedetti, P.R. Dudero, G. Franzoni, J. Haupt, K. Klapoetke, Y. Kubota, J. Mans, V. Rekovic, R. Rusack, M. Saserville, A. Singovsky

University of Mississippi, University, USA

L.M. Cremaldi, R. Godang, R. Kroeger, L. Perera, R. Rahmat, D.A. Sanders, D. Summers

University of Nebraska-Lincoln, Lincoln, USA

K. Bloom, S. Bose, J. Butt, D.R. Claes, A. Dominguez, M. Eads, J. Keller, T. Kelly, I. Kravchenko, J. Lazo-Flores, C. Lundstedt, H. Malbouisson, S. Malik, G.R. Snow

State University of New York at Buffalo, Buffalo, USA

U. Baur, A. Godshalk, I. Iashvili, S. Jain, A. Kharchilava, A. Kumar, S.P. Shipkowski, K. Smith

Northeastern University, Boston, USA

G. Alverson, E. Barberis, D. Baumgartel, O. Boeriu, M. Chasco, S. Reucroft, J. Swain, D. Wood, J. Zhang

Northwestern University, Evanston, USA

A. Anastassov, A. Kubik, N. Odell, R.A. Ofierzynski, B. Pollack, A. Pozdnyakov, M. Schmitt, S. Stoynev, M. Velasco, S. Won

University of Notre Dame, Notre Dame, USA

L. Antonelli, D. Berry, M. Hildreth, C. Jessop, D.J. Karmgard, J. Kolb, T. Kolberg, K. Lannon, W. Luo, S. Lynch, N. Marinelli, D.M. Morse, T. Pearson, R. Ruchti, J. Slaunwhite, N. Valls, J. Warchol, M. Wayne, J. Ziegler

The Ohio State University, Columbus, USA

B. Bylsma, L.S. Durkin, J. Gu, C. Hill, P. Killewald, K. Kotov, T.Y. Ling, M. Rodenburg, G. Williams

Princeton University, Princeton, USA

N. Adam, E. Berry, P. Elmer, D. Gerbaudo, V. Halyo, P. Hebda, A. Hunt, J. Jones, E. Laird, D. Lopes Pegna, D. Marlow, T. Medvedeva, M. Mooney, J. Olsen, P. Piroué, X. Quan, H. Saka, D. Stickland, C. Tully, J.S. Werner, A. Zuranski

University of Puerto Rico, Mayaguez, USA

J.G. Acosta, X.T. Huang, A. Lopez, H. Mendez, S. Oliveros, J.E. Ramirez Vargas, A. Zatserklyaniy

Purdue University, West Lafayette, USA

E. Alagoz, V.E. Barnes, G. Bolla, L. Borrello, D. Bortoletto, A. Everett, A.F. Garfinkel, Z. Gecse, L. Gutay, Z. Hu, M. Jones, O. Koybasi, M. Kress, A.T. Laasanen, N. Leonardo, C. Liu, V. Maroussov, P. Merkel, D.H. Miller, N. Neumeister, I. Shipsey, D. Silvers, A. Svyatkovskiy, H.D. Yoo, J. Zablocki, Y. Zheng

Purdue University Calumet, Hammond, USA

P. Jindal, N. Parashar

Rice University, Houston, USA

C. Boulahouache, V. Cuplov, K.M. Ecklund, F.J.M. Geurts, J.H. Liu, B.P. Padley, R. Redjimi, J. Roberts, J. Zabel

University of Rochester, Rochester, USA

B. Betchart, A. Bodek, Y.S. Chung, R. Covarelli, P. de Barbaro, R. Demina, Y. Eshaq, H. Flacher, A. Garcia-Bellido, P. Goldenzweig, Y. Gotra, J. Han, A. Harel, D.C. Miner, D. Orbaker, G. Petrillo, D. Vishnevskiy, M. Zielinski

The Rockefeller University, New York, USA

A. Bhatti, R. Ciesielski, L. Demortier, K. Goulianatos, G. Lungu, C. Mesropian, M. Yan

Rutgers, the State University of New Jersey, Piscataway, USA

O. Atramentov, A. Barker, D. Duggan, Y. Gershtein, R. Gray, E. Halkiadakis, D. Hidas, D. Hits, A. Lath, S. Panwalkar, R. Patel, A. Richards, K. Rose, S. Schnetzer, S. Somalwar, R. Stone, S. Thomas

University of Tennessee, Knoxville, USA

G. Cerizza, M. Hollingsworth, S. Spanier, Z.C. Yang, A. York

Texas A&M University, College Station, USA

J. Asaadi, R. Eusebi, J. Gilmore, A. Gurrola, T. Kamon, V. Khotilovich, R. Montalvo, C.N. Nguyen, I. Osipenkov, J. Pivarski, A. Safonov, S. Sengupta, A. Tatarinov, D. Toback, M. Weinberger

Texas Tech University, Lubbock, USA

N. Akchurin, J. Damgov, C. Jeong, K. Kovitanggoon, S.W. Lee, Y. Roh, A. Sill, I. Volobouev, R. Wigmans, E. Yazgan

Vanderbilt University, Nashville, USA

E. Appelt, E. Brownson, D. Engh, C. Florez, W. Gabella, W. Johns, P. Kurt, C. Maguire, A. Melo, P. Sheldon, S. Tuo, J. Velkovska

University of Virginia, Charlottesville, USA

M.W. Arenton, M. Balazs, S. Boutle, M. Buehler, S. Conetti, B. Cox, B. Francis, R. Hirosky, A. Ledovskoy, C. Lin, C. Neu, R. Yohay

Wayne State University, Detroit, USA

S. Gollapinni, R. Harr, P.E. Karchin, P. Lamichhane, M. Mattson, C. Milstène, A. Sakharov

University of Wisconsin, Madison, USA

M. Anderson, M. Bachtis, J.N. Bellinger, D. Carlsmith, S. Dasu, J. Efron, L. Gray, K.S. Grogg, M. Grothe, R. Hall-Wilton¹, M. Herndon, P. Klabbers, J. Klukas, A. Lanaro, C. Lazaridis, J. Leonard, R. Loveless, A. Mohapatra, D. Reeder, I. Ross, A. Savin, W.H. Smith, J. Swanson, M. Weinberg

†: Deceased

1: Also at CERN, European Organization for Nuclear Research, Geneva, Switzerland

2: Also at Universidade Federal do ABC, Santo Andre, Brazil

3: Also at Laboratoire Leprince-Ringuet, Ecole Polytechnique, IN2P3-CNRS, Palaiseau, France

4: Also at Suez Canal University, Suez, Egypt

5: Also at Fayoum University, El-Fayoum, Egypt

6: Also at Soltan Institute for Nuclear Studies, Warsaw, Poland

7: Also at Massachusetts Institute of Technology, Cambridge, USA

8: Also at Université de Haute-Alsace, Mulhouse, France

- 9: Also at Brandenburg University of Technology, Cottbus, Germany
- 10: Also at Moscow State University, Moscow, Russia
- 11: Also at Institute of Nuclear Research ATOMKI, Debrecen, Hungary
- 12: Also at Eötvös Loránd University, Budapest, Hungary
- 13: Also at Tata Institute of Fundamental Research - HECR, Mumbai, India
- 14: Also at University of Visva-Bharati, Santiniketan, India
- 15: Also at Facoltà Ingegneria Università di Roma "La Sapienza", Roma, Italy
- 16: Also at Università della Basilicata, Potenza, Italy
- 17: Also at Laboratori Nazionali di Legnaro dell' INFN, Legnaro, Italy
- 18: Also at Università degli studi di Siena, Siena, Italy
- 19: Also at California Institute of Technology, Pasadena, USA
- 20: Also at Faculty of Physics of University of Belgrade, Belgrade, Serbia
- 21: Also at University of California, Los Angeles, Los Angeles, USA
- 22: Also at University of Florida, Gainesville, USA
- 23: Also at Université de Genève, Geneva, Switzerland
- 24: Also at Scuola Normale e Sezione dell' INFN, Pisa, Italy
- 25: Also at INFN Sezione di Roma; Università di Roma "La Sapienza", Roma, Italy
- 26: Also at University of Athens, Athens, Greece
- 27: Also at The University of Kansas, Lawrence, USA
- 28: Also at Institute for Theoretical and Experimental Physics, Moscow, Russia
- 29: Also at Paul Scherrer Institut, Villigen, Switzerland
- 30: Also at University of Belgrade, Faculty of Physics and Vinca Institute of Nuclear Sciences, Belgrade, Serbia
- 31: Also at Gaziosmanpasa University, Tokat, Turkey
- 32: Also at Adiyaman University, Adiyaman, Turkey
- 33: Also at Mersin University, Mersin, Turkey
- 34: Also at Izmir Institute of Technology, Izmir, Turkey
- 35: Also at Kafkas University, Kars, Turkey
- 36: Also at Suleyman Demirel University, Isparta, Turkey
- 37: Also at Ege University, Izmir, Turkey
- 38: Also at Rutherford Appleton Laboratory, Didcot, United Kingdom
- 39: Also at INFN Sezione di Perugia; Università di Perugia, Perugia, Italy
- 40: Also at Institute for Nuclear Research, Moscow, Russia
- 41: Also at Horia Hulubei National Institute of Physics and Nuclear Engineering (IFIN-HH), Bucharest, Romania
- 42: Also at Istanbul Technical University, Istanbul, Turkey